

SOME ASPECTS OF THE RADIATION CHEMISTRY  
OF AQUEOUS SOLUTIONS OF NITROUS OXIDE

by

DAVID ALAN HEAD

B.Sc., University of British Columbia, 1965

A THESIS SUBMITTED IN PARTIAL FULFILMENT  
OF THE REQUIREMENTS FOR THE DEGREE OF  
MASTER OF SCIENCE  
in the Department

of

Chemistry

We accept this thesis as conforming to the  
required standard

THE UNIVERSITY OF BRITISH COLUMBIA

May, 1967

In presenting this thesis in partial fulfilment of the requirements for an advanced degree at the University of British Columbia, I agree that the Library shall make it freely available for reference and study. I further agree that permission for extensive copying of this thesis for scholarly purposes may be granted by the Head of my Department or by his representatives. It is understood that copying or publication of this thesis for financial gain shall not be allowed without my written permission.

Department of Chemistry

The University of British Columbia  
Vancouver 8, Canada

Date May 28, 1967

ABSTRACT

Deaerated acidic, neutral, and basic aqueous  $N_2O$  solutions were irradiated with Co-60  $\gamma$ -rays in order to: 1) determine the primary yields, and 2) resolve anomalies in relative rate constant ratios of the type  $k(e_{aq}^- + S)/k(e_{aq}^- + N_2O)$ . The yields of the gaseous products  $N_2$ ,  $O_2$ , and  $H_2$  were determined as a function of both pH and  $[N_2O]$ . About  $10^{-2}$  M  $N_2O$  is commonly used to evaluate relative rate constant ratios, but this  $[N_2O]$  scavenges not only hydrated electrons ( $e_{aq}^-$ ) but also another species, X, (where  $G(X) = 0.65 \pm 0.1$ ), resulting in erroneous rate constant ratios. Yields of primary species found were:  $G_{e_{aq}^-} = 2.4 \pm 0.1$ ,  $G_{H_2O^*} \sim 1.6$ , and  $G_{H_2^+} = 0.35 \pm 0.05$ .

Kinetic competition studies of the reaction of  $N_2O$  and  $H^+$  with  $e_{aq}^-$  were undertaken in the concentration ranges  $3 \times 10^{-5}$  to  $2 \times 10^{-4}$  M  $H^+$  and  $10^{-4}$  to  $10^{-3}$  M  $N_2O$ . The results cannot be explained by: 1) simple competition; 2) charge transfer, or 3) two species being scavenged. They may be explained

by assuming a conversion of  $N_2O$  to another species in acid solution. This acid species, suggested to be  $H_2N_2O_2$ , is apparently five times less reactive toward  $e_{aq}^-$  than is  $N_2O$  in neutral solution.

Deaerated neutral  $N_2O$  solutions were irradiated at extremely high intensity with very short pulses of 0.52 Mev electrons. The yields of the gaseous products  $N_2$ ,  $O_2$ , and  $H_2$  were studied in order to examine an expected decrease in solute products, and to determine primary yields at high dose rates. As predicted, significant scavenging occurs for high dose rates only at  $N_2O$  concentrations an order of magnitude larger than those at low dose rates. Also the scavenging, which is complete at  $\sim 10^{-2}$  M  $N_2O$  for low intensity irradiations, is not complete at  $2.6 \times 10^{-2}$  M  $N_2O$  for high intensity irradiations. These results indicate that the radiation yield of scavengable hydrated electrons is significantly larger at the high intensity used. The yield of hydrogen in pure water ( $G(H_2) = 1.15 \pm 0.2$ ) can be explained on the basis of inter-spur reactions of  $e_{aq}^-$ , H, and OH.

TABLE OF CONTENTS

	Pages
INTRODUCTION	
1. The Interaction Of Radiation With Matter	1-10
(a) Electromagnetic Radiation ( $10^3$ ev or more)	1-5
(i) the photoelectric effect	1-2
(ii) the Compton effect	2-3
(iii) pair production	3-4
(iv) coherent scattering	4
(v) photonuclear reactions	4-5
(b) Electrons	5-10
(i) radiation energy loss	6-7
(ii) energy loss by inelastic collision	7-8
(iii) elastic scattering	8-9
(iv) electron range	9-10
2. Ionizing Radiations And Water	10-17
3. Dose Rate Effects	18-19
4. The Problem	19-23
EXPERIMENTAL	
1. Materials	24
2. Apparatus	24-27
(a) Irradiation Cells	24-25
(b) Radiation Sources	25-26
(i) $\gamma$ -rays - low intensity	25-26
(ii) electron accelerator - high intensity	26
(c) Gas Chromatography	26-27
(d) pH Measurement	27
(e) Vacuum System	27
3. Procedures	27-31
(a) Cleaning	27-28
(i) pyrex cells	27-28
(ii) stainless steel cell	28
(b) Sample Preparation	28-29
(i) aqueous solutions	28-29
(ii) cyclohexane	29

(c) Degassing	29-30
(i) aqueous solutions	29-30
(ii) cyclohexane	30
(d) Analysis	30-31
4. Dosimetry	31-37
(a) The Fricke Dosimeter	31-33
(b) The Cyclohexane Dosimeter	33-36
(c) Faraday Cup	36-37

## RESULTS AND DISCUSSIONS

1. Cobalt-60 $\gamma$ Radiolysis	38-59
(a) Neutral Solutions	39
(b) Basic Solutions	39-43
(i) pH 13	42
(ii) pH 11.2	42-43
(c) pH 1.0	43-44
(d) Weakly Acidic Solutions	44-51
(i) simple competition model	44-46
(ii) charge transfer model	46-48
(iii) H-atom scavenging model	48
(iv) solute change model	48-51
(e) The Nature Of X	51-59
(i) the hyponitrous acid hypothesis	51-57
(ii) the hydration shell hypothesis	57-59
2. Electron Irradiations	59-68
(a) Diffusion Calculations	59-62
(b) Nitrogen Yields	62-65
(c) Hydrogen Yields	65-66
3. Conclusions	66-68

REFERENCES	68-73
------------	-------

## ILLUSTRATIONS

LIST OF TABLES

	Page
Table I: Comparison Of Absolute Values Of $k_{15}$ Determined From Relative Rate Constant Data	21
Table II: H-atom And $e_{aq}^-$ Yields For A Variety Of Systems	40
Table III: Simple Competition Model Calculations	46
Table IV: Charge Transfer Model Calculations	47
Table V: Comparison Of Some Of The Properties Of $CO_2$ And $N_2O$	52
Table VI: Some Properties Of Carbonic Acid And Hyponitrous Acid	53
Table VII: The Absorption Maxima Of $H_2N_2O_2$ , $HN_2O_2^-$ , And $N_2O_2^{=}$	55
Table VIII: The Solubility Of Both Nitrous Oxide And Carbon Dioxide	56
Table IX: Spur Overlap Calculations	61

LIST OF ILLUSTRATIONS

Figure 1: a) Pyrex reaction vessel for  $\gamma$ -irradiations.

b) Vessel for electron irradiations.

Figure 2: a) Cell for transfer of gases from vacuum line to gas chromatograph.

b) Cross-section of Faraday cup used.

Figure 3: Typical chromatogram.

Figure 4: Nitrogen yields as a function of nitrous oxide concentration at various pH values for Co-60  $\gamma$ -irradiations.

Figure 5: Reciprocal nitrogen yields as a function reciprocal nitrous oxide concentrations for Co-60  $\gamma$ -rays.

Figure 6: Mean  $[N_2O]/G(N_2)$  as a function of hydrogen ion concentration.

Figure 7: Nitrogen yields as a function of nitrous oxide concentration for electron irradiations.

Figure 8: Hydrogen yields as a function of nitrous oxide concentration for electron irradiations.

Figure 9: Fricke Dosimetry Plot.



I wish to thank Dr. D.C. Walker for his assistance in the preparation of this thesis. Without his comments and criticisms the maturing of this work could never have occurred. He has taught me the scientific method.

I am indebted to the B.C. Cancer Institute for use of their cobalt-60 source, and the time its staff gave to assist me in my experimentation.

I am grateful to Mr. E.A. Shaede for lessons in the operation of FÉBÉ.

## INTRODUCTION

### 1. The Interaction Of Radiation With Matter<sup>1</sup>

#### (a) Electromagnetic Radiation (1000 ev or more)

Not all photons incident upon a finite thickness of material will interact with that material, and those which undergo no interaction are changed in neither direction nor energy. The effect of matter upon electromagnetic radiation then is a reduction of intensity of that radiation. This reduction of intensity by absorption in matter of thickness  $x$  is given by

$$I = I_i e^{-ux} \quad (i)$$

where  $I$  is the transmitted and  $I_i$  the incident intensity of the radiation. The linear absorption coefficient,  $u$ , of the material is a constant dependent upon both the energy of the photon and the nature of the material. When they do interact with the material the photons tend to lose their energy in relatively large amounts.

The effect of absorbed photons upon matter may be one of five processes. These are: coherent scattering, the photoelectric effect, the Compton process, pair production, and photonuclear reactions. The relative probability of each process is dependent upon the energy of the photon.

#### (i) the photoelectric effect

Absorption of low energy photons occurs mainly by the photoelectric effect. A direct collision between the photon and one electron of an atom in the material

results in an electron being ejected from this atom with kinetic energy  $T$  given by

$$T = h\nu - \phi \quad (\text{ii})$$

where the incident photon energy is  $h\nu$  and  $\phi$  is the binding energy of the electron in the atom. This binding energy need not be equal to the ionization potential of the atom. Indeed with certain metals  $\phi$  may be decidedly less than the ionization potential<sup>2</sup>.

Since conservation of energy and momentum is made possible by the recoil of the remainder of the atom, this process is impossible with a free electron. In general the photoelectric effect increases with atomic number and decreases as the photon energy increases. The direction of the photoelectron is predominately at right angles to the direction of the incident photon at low energies, but this angle deteriorates toward zero as the energy is increased.

When an electron is ejected from an inner shell, the vacancy will be filled by an electron from an outer shell. This will give rise either to a low energy Auger electron, or to characteristic x-rays.

#### (ii) the Compton effect

Whereas the photoelectric effect can occur with a bound electron only, no such restriction is placed upon the Compton process. The entire photon energy is not given to the electron as it is in the photoelectric

effect. The incident photon is scattered with altered energy,  $E$ , at an angle  $\theta$  to the incident direction, while a recoil electron with energy  $T$  is formed at an angle  $\omega$ . The energy relationship is given by

$$E_0 = E + T \quad (\text{iii})$$

where  $E_0$  is the energy of the incident photon. The angular relations are dependent upon the energies involved. For example, the angle  $\theta$  may be found from the equation

$$E_0/E = (E_0/m_0c^2)(1 - \cos \theta) + 1 \quad (\text{iv})$$

where  $m_0c^2$  is the rest energy of the electron. For large incident photon energies  $\theta$  tends to be small, but increases as the energy decreases. Compton interactions will predominate for photon energies between one and five Mev for materials of high atomic number, and over a larger range for low atomic number materials. For example, in water the Compton interactions predominate from about 30 kev to 20 Mev.

#### (iii) pair production

When a photon is completely absorbed in the vicinity of an atomic nucleus, two particles, an electron and a positron, are set in motion. This process is called pair production. From conservation of energy we may write

$$E_0 = E_e + E_p + 2m_0c^2 \quad (\text{v})$$

which is almost exact since the nucleus acquires a negligible amount of energy. Since the energy that

is associated with an electron or a positron at rest is  $m_0 c^2 = 0.51 \text{ Mev}$ , pair production occurs only at photon energies greater than 1.02 Mev.

The positron which is formed is slowed down by the material and eventually combines with an electron of the material. This gives rise to two 0.51 Mev  $\gamma$ -rays, emitted in opposite directions.

#### (iv) coherent scattering

A photon may be scattered by interaction with atomic electrons. Since the electrons of an atom do not move independently of one another, the radiation that is scattered by one electron may interfere with that scattered by another electron. This type of scattering is called coherent, in contrast to Compton scattering which, since it involves a "free" electron and thus random phase relations, is incoherent.

Coherent scattering increases as the atomic number of the scattering material increases, and it occurs mostly at low photon energies. Since the energy range in which this coherent scattering occurs is the range in which the photoelectric effect is most efficient, then this effect is a minor one, which may often be neglected.

#### (v) photonuclear reactions

At high photon energies a proton or neutron may be ejected from the nucleus of the atom. A threshold

energy for this process is characteristic; this threshold is  $\sim 8$  Mev for high Z materials, and 10 to 15 Mev for low Z materials. The cross-section for these reactions is zero below the threshold, rises sharply beyond the threshold to a maximum at 3 to 6 Mev beyond it, and then falls as the energy increases further. This photonuclear cross-section is small compared to the Compton and pair production cross-sections at the same energy. However the ejected proton or neutron may be of some significance.

(b) Electrons

Energy is lost by electrons as they pass through matter by a variety of processes. These processes include excitation of atoms, radiation production, collisions with nuclei and electrons, resonance absorption, and electrodisintegration of nuclei. The relative importance of these processes is strongly dependent upon the energy of the incident electrons, and to some extent upon the nature of the absorbing material. At high energies radiation production and collisions which produce ionized and excited atoms predominate. At lower energies inelastic collisions and elastic scattering are of the greatest importance. This discussion will be limited to these important energy losing processes - namely radiation production, inelastic collision and excitation, and elastic

scattering.

(i) radiation energy loss

When a fast electron is decelerated by a nuclear field, electromagnetic energy (bremsstrahlung) must be radiated to conserve energy. Momentum is conserved by the action of the nucleus. The rate of energy loss per unit path length is approximately proportional to  $z^2 Z^2 m^{-2}$ , where  $z$  and  $Z$  are the charges on the particle and the nucleus respectively, and  $m$  is the mass of the decelerated particle. Greatest energy losses occur for the lightest particles and the highest atomic number materials. Since the intensity distribution of the bremsstrahlung is approximately constant as a function of electron energy<sup>3</sup>, large energy losses are equally as probable as small energy losses.

The kinetic energy lost by an electron of incident energy  $E$ , due to the decelerating field of nuclei and atomic electrons, where

$$m_0 c^2 \ll E \ll m_0 c^2 Z^{-1/3},$$

the screening effect of the atomic electrons of the nuclear field may be neglected, is given by<sup>4,5</sup>

$$-(dE/dx)_{\text{rad}} = (NEZ[Z+1]e^4/137 m_0^2 c^4) \\ (4 \ln [2E/m_0 c^2] - 4/3) \quad (\text{vi})$$

where  $N$  is the number of atoms per cubic centimeter.

When  $E \gg 137 m_0 c^2 Z^{-1/3}$  the screening is assumed to be complete, and equation (vi) becomes

$$-(dE/dx)_{\text{rad}} = (NEZ[Z + \zeta]e^4/137 m_o^2 c^4) (4 \ln [183/Z^{1/3}] + 2/9) \quad (\text{vii})$$

where  $\zeta$  is a measure of the amount of shielding, and is a function of atomic number.  $\zeta$  ranges from 1.4 for low atomic numbers to 1.1 for high atomic numbers.

Below 100 kev bremsstrahlung emission is negligible for electrons, but it increases rapidly with increasing energy. It predominates between 10 and 100 Mev, depending upon the stopping materials. The energy spectrum of bremsstrahlung extends from zero to the energy of the incident electrons, and is in fact the continuous x-ray spectrum. Bremsstrahlung does not produce any significant changes in the stopping material unless subsequently absorbed.

(ii) energy loss by inelastic collision

Energy may be lost by charged particles by means of Coulombic interactions (inelastic collisions) with the electrons of the stopping material. Collisions of this type, which produce excitation and ionization in the stopping material, are the dominant processes whereby electrons are thermalized at incident energies below those at which bremsstrahlung emission occurs. This energy loss by excitation and ionization is given by <sup>4,6</sup>

$$-(dE/dx)_{\text{coll}} = (2\pi Ne^4 Z/m_o v^2) [\ln(m_o v^2 E/2I^2 [1 - \beta^2]) - (2\sqrt{1 - \beta^2} - 1 + \beta^2) \ln 2 + 1 - \beta^2 + 1/8(1 - \sqrt{1 - \beta^2})^2] \quad (\text{viii})$$



where  $E$  is the relativistic kinetic energy,  $x$  the path length,  $N$  the number of atoms per cubic centimeter,  $Z$  the nuclear charge, and  $I$  the average ionization potential of the atom. This expression includes the assumption that the most energetic electron after the collision is the bombarding electron.

The average ionization potential of the material takes into account the effect of the binding energies on the loss of energy.  $I$  may be determined either by experiment

$$I = kZ \quad (\text{ix})$$

where  $8 < k < 16$  and is a constant for each element, or by calculation

$$Z \ln I \sim \sum f_i \ln I_i \quad (\text{x})$$

where  $f_i$  is the number of electrons in shell  $i$ , and  $I_i$  is the ionization potential of that shell.

For an electron of energy  $E$  Mev, the ratio of the energy lost by collisions to that lost by radiation is

$$\frac{(dE/dx)_{\text{coll}}}{(dE/dx)_{\text{rad}}} \sim 1600 m_0 c^2 / EZ \quad (\text{xi})$$

### (iii) elastic scattering

Charged particles may be deflected by the electrostatic field of an atomic nucleus. Since their mass is so small, electrons may be deflected in this manner quite easily. The Rutherford formula for the scattering of electrons through an angle  $\phi$  in the solid angle  $2\pi$

(which neglects the effect of orbital electrons) is

$$d\phi = (\pi e^4 Z^2 / 2m_0^2 v^4) (\sin \theta / \sin^4 [\theta/2]) d\theta \quad (\text{xii})$$

However only large angle scattering of electrons follows this formula closely. The scattering is greatest for low energies and for materials of high atomic number.

#### (iv) electron range

A charged particle will undergo a large number of small energy losses in its path through the medium. Since the electron has a relatively low mass, the scattering and the variation in the energy lost is larger than for other charge particles. The statistical variation in its total energy loss is, however, small. Thus a range of electrons is still approximately well defined. The percentage of transmitted electrons as a function of absorber thickness for monoenergetic electrons is a rapidly decreasing linear curve with a tail. The absolute maximum range,  $R_0$ , is the point at which the tail disappears into the background, and may be calculated by integration of the collisional energy loss.

$$R_0 = \int_0^E dE / (dE/dx) \quad (\text{xiii})$$

Radiation energy losses do not effect the absolute maximum range, since they are infrequent, and usually involve large energy losses by a few electrons.

The extrapolated or practical maximum range,  $R_p$ ,

is found by extrapolating the linear portion of the curve until it intersects with the background. Both of these ranges are characteristic of the original electron energy. The difference is essentially due to multiple scattering.

A linear extrapolation is not possible when a continuous, rather than a monoenergetic, spectrum of electron energies exists. The range,  $R$ , is then ordinarily taken as that point at which the absorption curve merges with the background. This range is similar in definition to the absolute maximum range,  $R_0$ . For energies from 0.01 to 2.5 Mev the following empirical equation holds when aluminum is the stopping material<sup>7</sup>

$$R \text{ (or } R_0) = 412 E^n \quad (\text{xiv})$$

where  $n = 1.265 - 0.0954 \ln E$ , and  $R$  (or  $R_0$ ) has units of  $\text{mg/cm}^2$ , while  $E$  is the maximum (or monoenergetic) energy.

## 2. Ionizing Radiations And Water

"When x-rays or  $\gamma$ -rays pass through a substance, the main result is the formation of secondary electrons, which cause the chemical change."<sup>8</sup> Only the Compton effect and the photoelectric process are of any chemical significance when ionizing electromagnetic radiations strike water. That is to say these effects are the only ones whose interactions with water will effect that water in such a way as to result in a net chemical

change. Photonuclear reactions are not of importance, since the energy of the radiations most often used is below the threshold for this process. Coherent scattering is a negligibly important process, and in any case the effect is more upon the radiation than on the stopping material. Pair production results in net chemical only if the two 0.51 Mev  $\gamma$ -rays formed are subsequently absorbed in either a Compton or a photoelectric process by the water.

"Whether the incident radiation is penetrating electromagnetic radiation, such as  $\gamma$ -rays, or such charged particles as  $\beta$ -rays or an electron beam from a high voltage machine the agency which effects the water is always the same, namely, a fast-moving electron."<sup>9</sup> The question of the nature of this effect then arises. As has earlier been noted, a fast electron loses its energy in a variety of ways, the most important of which are elastic scattering, inelastic collisions, and radiation production. Only inelastic collisions have an effect upon water. This effect is that water may either be raised to an excited state, or be ionized.

The primary electron gives rise to secondary ionizations and excitations along its track as it is slowed by the water. As is evident from equation (viii) the rate of energy loss varies in some inverse relation with the velocity, and hence the energy, of the electron.

The rate of energy loss is commonly discussed in terms of linear energy transfer (abbreviated as L.E.T.). The L.E.T. is increasing as the electron loses energy. The number of ionizations and excitations will therefore increase as the electron slows down, and they will, in general, occur closer together.

Consider the electrons formed in these secondary ionizations. The secondary electron may itself give rise to another, tertiary, electron. Tertiary excitations would occur as well. In general, the secondary electron will have much less energy than the primary. As a first order approximation we may categorize these secondary electrons in two ways: 1) less-energetic, with less than 100 ev of energy; and 2) more-energetic, with energy of 100 ev or more.

The less-energetic secondary electrons will have quite a short range. Their path, due to multiple deflections, will not be a straight line, but will be bound in some more or less spherical region. The result is an approximately spherical cluster of secondary ionizations and excitations known as a spur.

The more-energetic secondary electrons will have the range to form true tracks of their own. These tracks, branching from the track of the primary, would be of similar structure to the primary track. This type of track is known as a  $\delta$ -ray.

Of course this rather naive division of the sec-

ondary electrons into two categories will result in a simplification of a rather more complex situation. The situation will be radically different at the extremes of the divisions. It would perhaps be enlightening to consider these extreme cases.

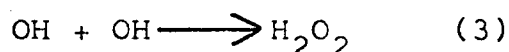
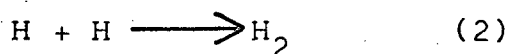
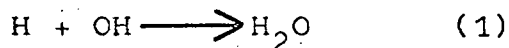
A theoretical development of this situation has been done by Mozumder and Magee <sup>10</sup>. They considered that a highly energetic  $\delta$ -electron will be as pictured above. It will generate its own track, much like the primary. The average separation of the spurs will be such that they are non-overlapping, since for very energetic electrons the L.E.T. is low. For a 0.50 Mev electron the mean separation of the spurs is of the order of  $10^3$  to  $10^4$  Å <sup>11,12</sup>, while the size of the spur upon formation is estimated to be of the order of 20 Å <sup>12,13,14</sup>. The track of this sort of  $\delta$ -electron is known as a BRANCH TRACK, and occurs at energies above  $\sim 5000$  ev.

As the energy of the  $\delta$ -electron falls the L.E.T. increases and the spurs are formed closer together. When the energy falls below  $\sim 5000$  ev the spurs begin to overlap. A track with overlapping spurs such as this is called a SHORT TRACK, and arises from a  $\delta$ -electron of  $\sim 500$  to 5000 ev.

Decreasing the energy still further, a point is finally reached where  $\delta$ -electron will have insufficient energy to escape the site of its formation.

The secondary (and higher order) electrons formed will also be unable to escape this area. The result is a super-spur known as a BLOB. This blob may be shaped more like a pear than a sphere, since the formation of the spurs will be greater as the  $\delta$ -electron is stopped. The energy limits for blobs will be  $\sim 100$  ev to 500 ev. Below 100 ev the spurs formed are still considered to be isolated events. The energy limits that have been set for the branch tracks, short tracks, blobs, and spurs are not to be interpreted as rigid barriers, but rather as general lines of demarcation.

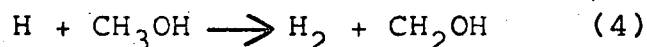
The consideration of the distribution of the species formed, whether they be blobs, spurs, or whatever, must lead to a consideration of the identity of these species. Since the electrons may lose their energy by excitation of the media, one of the species formed is  $\text{H}_2\text{O}^*$ . This excitation may be sufficient to decompose the water but not ionize it. Species such as  $\text{H}^*$  and  $\text{OH}^*$  are formed. These species are not unknown<sup>15,16,17</sup>. The OH and H radicals might of course recombine within the spur



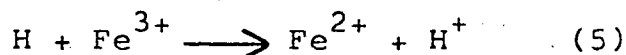
and so molecular hydrogen and hydrogen peroxide must be added to our list.

Until about 1958 these species were sufficient to

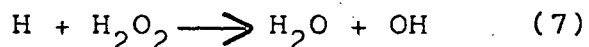
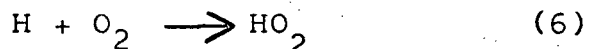
describe quite adequately all of the radiation chemistry of water. Indeed the diffusion model of Samuel and Magee <sup>12,13</sup>, which dealt only with H and OH, was considered fundamentally sound, with errors only in minor detail. However in 1958 Baxendale and Hughes <sup>18</sup> found that hydrogen produced in irradiated acidified aqueous methanol solutions



was reduced by  $\text{Fe}^{3+}$  and  $\text{Cu}^{2+}$  ions by an amount that was considerably higher than the competition of (4) with (5)



would predict. About the same time Hayon and Weiss <sup>19</sup> found that in acidic solution low concentrations of monochloroacetic acid gave hydrogen as the predominant product, while at high concentrations, and in neutral and basic solution  $\text{Cl}^-$  ion was the favoured product. Barr and Allen <sup>20</sup> found that the rate constant ratio  $k_6/k_7$ , where



differed markedly when the H was radiation produced than when it was produced by another method. Czapski and Schwarz <sup>21</sup> found that the principle reducing species in irradiated water had a unit negative charge by varying the ionic strength and applying the Brønsted-Bjerrum theory and the extended Debye-Hückel

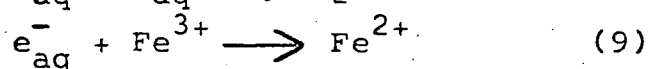
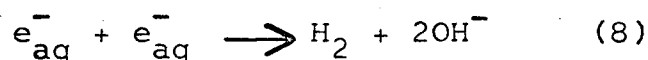


theory of electrolytes.

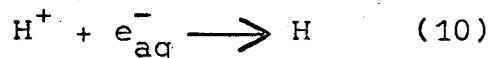
Boag and Hart<sup>22</sup> and Keene<sup>23</sup> found that pulse irradiated water exhibited an absorption spectrum much like that found for the solvated electron in liquid ammonia. The shape of the spectrum was remarkably similar, the major difference being that the  $\lambda_{\max}$  for water was  $\sim 7000 \text{ \AA}$ , while that for liquid ammonia was  $\sim 14,000 \text{ \AA}$ .

All this evidence pointed to the existence of another reducing species that up until this time had been mistaken for the hydrogen atom. It was the hydrated electron,  $e_{\text{aq}}^-$ , as predicted earlier by Platzman<sup>24</sup>. In fact this species is the principle reducing species in water irradiated either with cobalt-60  $\gamma$ -rays, or with fast electrons.

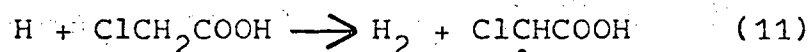
The reactions



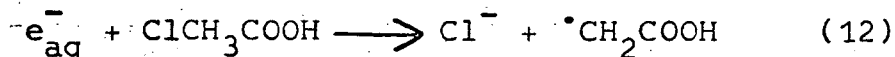
in competition would account for the observations of Baxendale and Hughes, since  $k_8/k_9$  is substantially less than  $k_4/k_5$ . In acid solution the expected fate of the hydrated electron is



The hydrogen atom so formed would be able to abstract another from monochloroacetic acid to give molecular hydrogen.



However at high concentrations of monochloroacetic acid reaction (12) competes with reaction (10)



to yield chloride ion. In neutral and basic solution reaction (12) predominates and  $Cl^-$  is the product there also, in agreement with the observations of Hayon and Weiss.

In pure water irradiated with cobalt-60  $\gamma$ -rays or fast electrons the yields of these species discussed above are approximately

$$\begin{array}{lll} G_{e_{aq}^-} = 2.5 & G_H = 0.6 & G_{OH} = 2.8 \\ G_{H_2O_2} = 0.8 & G_{H_2} \leq 1.2 & \end{array}$$

where  $G_X$  is the number of X molecules formed per 100 ev of energy absorbed by the solution.

After formation the fates of these species are generally two-fold; they may react with each other within the spur, or they may escape the spur by diffusion. If an escape by diffusion is to be their fate, then they must eventually encounter another diffusion species from another spur, react with solute molecules, or react with solvent molecules. These events are the chemistry of the irradiation. The relative importance of each of the products and of each reaction may in theory be predicted from the rates of diffusion and the rates of reaction. An example of such theoretical calculations are those by A. Kuppermann <sup>14</sup>.

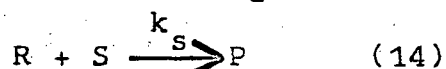
### 3. Dose Rate Effects

From the previous discussion it is evident that the chemical effect of ionizing radiation will depend upon the rate at which the ionization occurs in the aqueous medium. Since the chemical effects are due to species escaping from one spur meeting those escaping from another, or reacting with solute or solvent molecules, then the average separation of the spurs will greatly effect the fate of the average species. This density of spurs will depend upon the density with which they are formed, which is to say upon the intensity of the ionizing radiation. The chemical effect will be intensity or dose rate dependent.

Spur overlappings will result in an increased probability of radical-radical reactions to form the molecular products, and a decreased probability of radical-solute reactions. An increase in the molecular products ( $H_2$  and  $H_2O_2$ ) at the expense of the solute product should be found. Just such behaviour has been seen <sup>24,25,26</sup>.

A more rigorous derivation of this behaviour is shown in the following simple calculation <sup>27</sup>. Consider an irradiated solution such that there is formation of radicals R. These will be formed at a rate equal to  $G_R I$ , where I is the intensity of the radiation, and  $G_R$  is the number of radicals formed per 100 ev of energy absorbed. Radicals from different spurs will combine

only if there is an appreciable amount of R in the solution, else they will react with the solute only. If there is a large steady-state concentration of R the radicals may either react with S or themselves.



The rate of recombination is then  $k[R]^2$ , while the rate of the solute reaction is  $k_s[R][S]$ . Since the rate of formation must equal the rate of disappearance of the radicals

$$G_R I = k[R]^2 + k_s[R][S] \quad (xv)$$

and solving for [R]

$$[R] = -k_s[S]/2k + (k_s^2[S]^2/4k^2 + G_R I/k)^{1/2} \quad (xvi)$$

The yield of the product G(P) will show a similar dependence upon intensity.

$$G(P) \cdot I = k_s[R][S] \quad (xvii)$$

If  $k[R]^2$  is negligible the two yields are equal, but if this is not the case then we may write

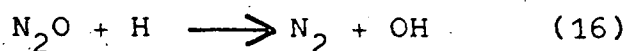
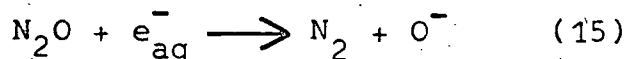
$$G(P) = (k_s^4[S]^4/4k^2 I^2 + k_s^2[S]^2 G_R/kI)^{1/2} - k_s^2[S]^2/2kI \quad (xviii)$$

The above expression relates the product yield to the intensity of the radiation. As we might see, the yield of product, G(P), will decrease as the intensity of the radiation increases.

#### 4. The Problem

One of the solutes that is commonly added to sol-

ution to react with one or more of the species formed by the radiation (called scavengers) is nitrous oxide. The reactions that it is said to undergo are <sup>15,28</sup>



The reactions of nitrous oxide give an easily distinguishable and measureable product, nitrogen gas. This product has the advantage of being quite stable. The rate constant for reaction (15) is at least  $5 \times 10^3$  times larger than that of reaction (16) <sup>29</sup>. Because of this large difference between  $k_{15}$  and  $k_{16}$  judicious use of  $\text{N}_2\text{O}$  can distinguish the radiation yields of H and  $\text{e}_{\text{aq}}^-$ . Thus nitrous oxide would seem to be an ideal scavenger to use in the radiolysis of aqueous media.

The situation, however, is far from ideal. The concentration of  $\text{N}_2\text{O}$  necessary to scavenge completely the hydrated electrons escaping the spurs was thought to be  $\sim 10^{-2} \text{ M}$  <sup>28</sup>. Solutions of this concentration should give  $G(\text{N}_2)$  values equal to  $G\text{e}_{\text{aq}}^-$ , whereas they yield  $G(\text{N}_2)$  values of  $\sim 2.9$  to  $3.1$  compared to  $G\text{e}_{\text{aq}}^-$  of  $\sim 2.4$  found in other systems. Since the value of  $k_{15}$  is  $\sim 10^{10} \text{ M}^{-1}\text{sec}^{-1}$  (found by pulse radiolysis), why is it necessary to have such a high concentration of  $\text{N}_2\text{O}$  to scavenge all spur-escaping  $\text{e}_{\text{aq}}^-$ ? The lifetime of  $\text{e}_{\text{aq}}^-$  with respect to  $\sim 10^{-2} \text{ M } \text{N}_2\text{O}$  is  $< 10^{-8}$  seconds, which is barely enough time for  $\text{e}_{\text{aq}}^-$  to escape the spur.

Table I shows some of the anomalies that have

TABLE I

Comparison Of Absolute Values Of  $k_{15}$  Determined From  
Relative Rate Constant Data

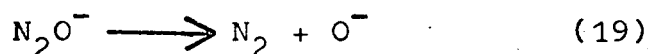
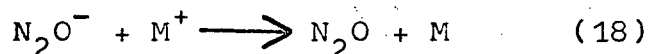
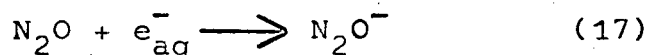
$k(e^-_{aq}+S)$ $k_{15}$	"S"	$k_{15}$ ( $\times 10^9 M^{-1} s^{-1}$ )	pH	$N_2O$ ( $\times 10^{-3} M$ )	ref.
0.8	$H^+$	$30 \pm 3$	3.0	14	28
$0.65 \pm 0.35^a$	$H^+$	$54 \pm 33$	2.7	1-6	15
$1.2 \pm 0.6^{a,b}$	$H^+$	$28 \pm 16$	1.8	3-20	15
$1.49 \pm 0.16^c$	$H^+$	$13 \pm 3$	1.7-2.7	9-19	35
1.64	$H^+$	$14 \pm 1.4$	1.2	2-23	31
$1.70 \pm 0.15$	$H^+$	$14 \pm 3$		16	30
$2.20^c$	$H^+$	$11 \pm 1$		"high"	32
$2.67 \pm 0.50$	$H^+$	$8.8 \pm 2.5$	3.1	3-15	33
$0.67 \pm 0.07$	acetone	$8.8 \pm 1.3$		16	30
$1.02^d$	acetone	$5.8 \pm 2.0$	5.9	5-10	31
$1.50^c$	acetone	$3.9 \pm 0.2$		"high"	32
$1.17 \pm 0.15$	$NO_3^-$	$9.4 \pm 2.4$		16	30
$2.86^c$	$NO_3^-$	$3.7 \pm 0.2$		"high"	32
$0.89 \pm 0.07$	$Fe(CN)_6^{3-}$	$3.4 \pm 0.8$		16	30
$1.20^c$	$Fe(CN)_6^{3-}$	$2.5 \pm 0.6$		"high"	32
$3.85 \pm 0.04$	$Cu^{2+}$	$8.7 \pm 1.5$		16	30
$0.46 \pm 0.04$	$CO_2$	$1.7 \pm 0.4$	3.5-4.0	16	30
$0.49 \pm 0.05$	$NO_2^-$	$9.4 \pm 1.0$		16	30
$0.19 \pm 0.01$	chloroacetate	$6.3 \pm 0.4$		16	30
$1.03^d$	acetaldehyde	3.4	5.9	10	31
$0.31 \pm 0.07$	$Te^{IV}$	$1.9 \pm 0.6$	13.2	20	34
pulse radiolysis	{	$8.67 \pm 0.6^f$	7	0.3-5	36
		$5.6 \pm 2.0$		23	37
		$5.6 \pm 2$	11	0-0.005	38

a.ferrocyanide present;b.ferricyanide present;c.photo-  
lysis;d.isopropanol present;e. $k(e^-_{aq}+S)$  values from ref.  
39, except  $Te^{IV}$  from ref. 43;f.methanol present.

arisen with the use of  $N_2O$ . In various systems very different relative rate ratios are found by different experimenters. When  $k_{15}$  is calculated using absolute rate constants obtained by pulse radiolysis techniques quite a range of values, too wide to be accounted for by experimental error, is found.

In earlier work <sup>40</sup> the yield of  $N_2$  as a function of  $[N_2O]$  was investigated, and it was found that about  $8 \times 10^{-5}$  M  $N_2O$  was sufficient to scavenge all the  $e_{aq}^-$  escaping the spurs. The yield of  $e_{aq}^-$  determined from  $G(N_2)$  was  $(2.45 \pm 0.1)$ . At  $\sim 10^{-2}$  M  $N_2O$ ,  $G(N_2)$  increased to 3.1. This increased radiation yield of  $0.65 \pm 0.1$  may result from either intra-spur scavenging of  $e_{aq}^-$ , or scavenging of a second radiation produced species - possibly the H-atom species which is believed to be formed with a yield given by  $G_{H\cdot} = 0.6$ . Much of the confusion in the relative rate constant ratios may stem from the use of higher concentrations of nitrous oxide than is necessary to scavenge  $e_{aq}^-$ .

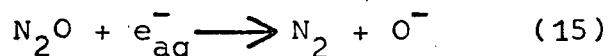
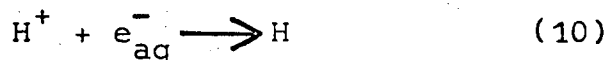
Dainton <sup>41</sup> and Anbar <sup>42</sup> have suggested that  $N_2O$  may undergo the following reactions.



Some of the difficulties and differences may be the result of this charge transfer mechanism.

The main aim of this work was to attempt to

resolve some of these difficulties. A simple competition



was to be studied at concentrations of nitrous oxide sufficiently low to avoid reaction (16) and at a pH large enough that  $\text{N}_2\text{O}$  would be able to compete with the proton effectively. Since the values of  $k_{15}$  and  $k_{10}$  are  $(8.67 \pm 0.6) \times 10^9$  and  $(2.36 \pm 0.24) \times 10^{10} \text{ M}^{-1} \text{sec}^{-1}$  respectively<sup>34</sup>, and the concentration of nitrous oxide must be less than  $\sim 2 \times 10^{-3} \text{ M}$ , the range of pH values needed to satisfy the necessary conditions was  $\sim 4$  to  $\sim 4.5$ .

The acquisition of a pulse electron accelerator able to give extremely high dose rates suggested a study of the aqueous nitrous oxide system at these high intensities. The predicted behaviour (an increase in molecular products and a decrease in solute products) might be tested. The yields of  $\text{N}_2$  would give information concerning  $\text{Ge}_{\text{aq}}^-$  at high intensities.



## EXPERIMENTAL

### 1. Materials

Laboratory distilled WATER was redistilled from acidified permanganate, then refluxed a minimum of 24 hours from alkaline permanganate before use. A Fricke dosimetry study showed no detectable organic material was present. NITROUS OXIDE gas, supplied by Matheson Of Canada, was purified by trap-to-trap distillation until a dynamic vacuum of at least  $2 \times 10^{-6}$  torr was achieved. A high resolution mass spectrometric analysis indicated that the gas was free from impurities. Three purities of CYCLOHEXANE were used. Phillips 66 research grade and B&A reagent grade were used without further purification; B&A reagent grade was also used after distillation, the middle third being collected. Analytical reagent SODIUM HYDROXIDE, SULPHURIC ACID, FERROUS AMMONIUM SULPHATE, and POTASSIUM CHLORIDE were used without further purification.

### 2. Apparatus

#### (a) Irradiation Cells

Irradiation of solutions by cobalt-60  $\gamma$ -rays was carried out in a cylindrical pyrex cell, internal diameter 22.4 mm and length  $\sim 110$  mm. A 50 ml round-bottomed pyrex flask was connected to the cell and served to hold the liquid during degassing. The cell terminated in a B14 cone by which it could be attached

to a vacuum tap; the tap could in turn be attached to the vacuum line. See figure 1(a).

Solutions irradiated by 0.52 Mev electrons were contained in a cylindrical stainless steel cell, 35 mm internal diameter, and 8 mm in depth. This is part C in figure 1(b). A pyrex window (D) was araldited onto the back of the cell to allow observation of the interior. An aluminium face plate (A) and a teflon ring (in the face of C) served to hold a metal foil (D) in place over the front of the cell. This foil could be changed between experiments, and acted as an electron window for the cell. Two such windows were used: 0.001" of aluminum and 0.002" of stainless steel. A pyrex round-bottomed flask (F), with a side arm terminating in a B14 cone, was araldited to the entrance port (E). A tap attached to the B14 cone was the means by which the cell could be placed on the vacuum line. The whole system was able to maintain a dynamic vacuum of  $\sim 10^{-6}$  torr. The system was attached to the front of the electron accelerator by the aluminum face plate (A).

#### (b) Radiation Sources

##### (i) $\gamma$ -rays - low intensity

A 1000 curie cobalt-60  $\gamma$ -ray source was used. This source was a therapeutic machine located at the B.C. Cancer Institute. Due to the design of this machine the cells could be placed no closer than  $\sim 50$  cm from the source, resulting in a low dose rate and, due to the

inverse square fall off, a variation of the dose through the cell of  $\sim 18\%$ . Solutions were irradiated in groups of six.

(ii) electron accelerator - high intensity

A Febetron pulse electron accelerator manufactured by the Field Emission Corp., McMinnville Oregon, was used to achieve high intensity irradiations. The energy of the electrons emerging from the tube window was a maximum of 0.52 Mev. The current of electrons striking the sample cell was  $\sim 250$  amperes. The pulse width at half-height was 30 nanoseconds.

(c) Gas Chromatography

An aerograph A-90-P2 gas chromatograph was used to analyse permanent gases. A twenty foot, 5 Å, molecular sieve column and a thermal conductivity detector with matched tungsten filaments were used. When helium was used as the carrier gas the limits of detection were as follows:

$$N_2 \sim 2 \times 10^{-9} \text{ moles(s)}$$

$$O_2 \sim 1 \times 10^{-9} \text{ moles(s)}$$

$$H_2 \sim 5 \times 10^{-8} \text{ moles(s)}$$

These limits are those for which the error in measurement was not excessively large. Detection of amounts of gases of one-fifth of these values was possible, but the error in their measurement was probably 50%. When argon was used as a carrier gas, the similarly defined limits were:

$$N_2 \sim 5 \times 10^{-8} \text{ moles}$$

$$O_2 \sim 3 \times 10^{-8} \text{ moles}$$

$$H_2 \sim 2 \times 10^{-9} \text{ moles}$$

It is evident from these two sets of limits that argon is the carrier gas to be used when the measurement of hydrogen is most important, while helium should be used when detection of oxygen or nitrogen is more important.

#### (d) pH Measurements

A Beckman Zeromatic II pH meter was used for all pH measurements. In addition all solutions were made up strictly by volume, thus ensuring a further check on the pH.

#### (e) Vacuum System

A hard vacuum was obtained in a pyrex glass system using a mercury diffusion pump backed by a rotary oil pump. The working pressure of the system was  $\sim 10^{-6}$  torr of permanent gases, as measured on an ionization sp guage.

### 3. Procedures

#### (a) Cleaning

##### (i) pyrex cells

Initially cells were washed with permanganic acid, rinsed twice with tap water, steamed from a solution of permanganate in acidified distilled water for at least fifteen minutes, heated in an oxy-gas

flame to just below the softening point of the glass, washed several times with doubly distilled water, and finally washed twice with triply distilled water.

After use the cells were left evacuated until needed again. In subsequent use only the steaming and washings with doubly and triply distilled water were employed.

(ii) stainless steel cell

In order to maintain the epoxy resin adhesive, it was not possible to steam, flame, or wash the cell with strong acid. The cell was washed initially with analar isopropanol. This was followed with several washings with triply distilled water. After use the cell was kept evacuated until needed again. In further usage only the washings were employed.

(b) Sample Preparation

(i) aqueous solutions

Acidic solutions were made with triply distilled water and sulphuric acid. Triply distilled water was used for neutral solutions. Sodium hydroxide and triply distilled water was used for basic solutions. When acidic or basic conditions were required an aliquot of the solution was taken and the pH measured on a pH meter.

The requisite volume of liquid was introduced into the cell via the B14 cone. This cone was then sealed to the B14 socket of the vacuum tap with either picein wax (pyrex cells) or Apezion N grease (stainless

steel cell). The volume of liquid used was 25 ml for the pyrex cell and ~ 10 ml for the stainless steel cell. The whole cell was then evacuated at room temperature. The liquid was degassed and the requisite amount of nitrous oxide introduced. If isopropanol was to be added, it was distilled into the solution at 77°K as a last step.

For high concentrations of nitrous oxide the gas was equilibrated with the liquid at a suitable pressure, a correction being made for the vapour pressure of the water. For concentrations so low that this equilibrium method was impractical, a known amount of gas was frozen into the solution at 77°K.

(ii) cyclohexane

The amount of cyclohexane required was introduced into the cell at the B14 cone. A B14 socket attached to a vacuum stopcock was joined to this cone and the cell was partially evacuated at room temperature. The cyclohexane was degassed.

(c) Degassing

(i) aqueous solutions

The freeze-pump-thaw technique was used to remove the major portion of the dissolved gases from the solution. In an earlier report <sup>40</sup> it was shown that this technique could leave up to 0.2  $\mu$ moles of gas in 25 ml of solution. But nitrous oxide, added to the solution to achieve the final reaction configuration,

was able to release some or all of this gas during the analysis process, depending upon the amount of nitrous oxide initially used. To overcome this difficulty, the amount of  $N_2O$  that was to be used in the reaction was introduced into the reaction vessel, allowed to equilibrate, and removed by a freeze-pump-thaw cycle. In this way the "residual" gas was removed prior to achieving the final reaction configuration. Furthermore the nitrous oxide was essentially all removed from the solution by the freeze-pump-thaw cycle, so that later additions of nitrous oxide would result in a concentration of gas that was known to a least five per cent.

(ii) cyclohexane

Liquid cyclohexane was degassed by multiple freeze-pump-thaw cycles at  $77^{\circ}K$  until the pressure of the system at that temperature was less than  $2 \times 10^{-6}$  torr, as indicated by an ionization guage.

(d) Analysis

The irradiated solution was exposed to two traps at  $77^{\circ}K$  in a system held at a high vacuum. The permanent gases were pumped from the traps into a McLeod guage by a small mercury diffusion pump. The amounts of gas measurable, with the corresponding estimate of the error, are given below.

20 to 0.05  $\mu$ moles ..... 5 to 10%

0.05 to 0.01  $\mu$ moles ..... 10 to 50%

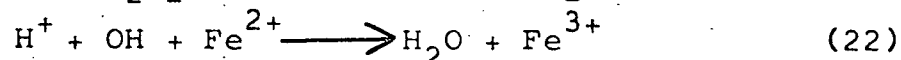
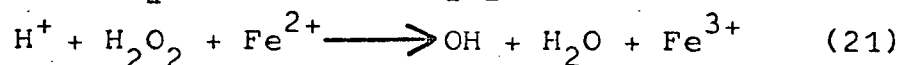
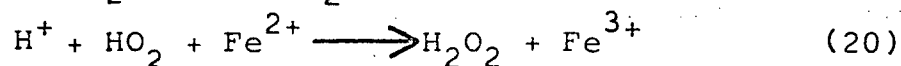
0.01 to 0.002  $\mu$ moles ..... 50 to 100 %

The gas was transferred from the McLeod to a gas burette, and from it to a small cell (figure 2[a]) by which it might be introduced into a gas chromatograph. The amounts of the individual gases were determined from the chromatogram, and the total compared with that measured by the McLeod. A typical chromatogram is shown in figure 3, indicating that a calibration accompanied each analysis. The errors in these measurements, when corrected for hold-back in the small mercury diffusion pump, typically was estimated to be less than ten per cent.

#### 4. Dosimetry

##### (a) The Fricke Dosimeter

The dose rate of the cobalt-60 source was determined by the Fricke dosimeter. This is a chemical dosimeter first proposed by Fricke<sup>56</sup> in 1927, and since then modified by Miller and others<sup>57</sup>. In this dosimeter an air saturated solution of  $\text{Fe}(\text{NH}_4)_2(\text{SO}_4)_2$  in 0.8 N sulphuric acid is irradiated. The reactions that occur are thought to be

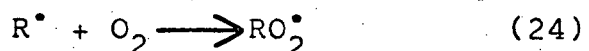
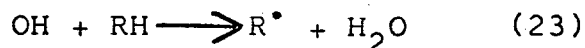


For cobalt-60  $\gamma$ -rays  $G(\text{Fe}^{3+}) = 15.5$ . The ferric ion is determined spectrophotometrically at 304 nanometers

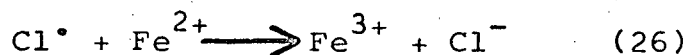
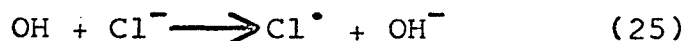


where the decadic molar extinction coefficient is 2174 at 20°C<sup>58</sup>.

When organic material is present in the solution the following reactions may occur



Since  $\text{RO}_2^\bullet$  is an organic analog of  $\text{HO}_2$ , it would also be able to oxidize three  $\text{Fe}^{2+}$  ions in reactions similar to (20), (21), and (22). The result would be an increased  $G(\text{Fe}^{3+})$ , which would lead to errors in the determination of the dose or the dose rate. Chloride ion is added to suppress this possibility. The reactions that may occur with  $\text{Cl}^-$  ion present are



Since the chloride ion is in high concentration relative to the organic impurity the fate of the OH will be reaction (25) rather than reaction (23). Since the  $\text{Cl}^\bullet$  has an effect on ferrous ion that is the equivalent of the effect of the OH, there will be no change in  $G(\text{Fe}^{3+})$ .

If oxygen is not present in the solution, then reactions (6) and (20) will not occur. The result is that  $G(\text{Fe}^{3+})$  becomes 8.2<sup>59</sup>. This will mean that the yield of ferric ion as a function of irradiation time will be non-linear for a solution in which the oxygen has become depleted.

Two series of Fricke dosimetry studies were undertaken, the first some seventeen months prior to the second. The dosimetry curve for the first study is shown in figure 9. A similar curve was obtained for the second study. The dose rates, determined from the slopes of the optical density versus irradiation time curves, were  $(2.8 \pm 0.1) \times 10^{17}$  and  $(2.2 \pm 0.1) \times 10^{17}$  ev/l-sec. for the first and second study respectively. Application of the decay equation,

$$R = R_0 e^{-t/\lambda} \quad (\text{xix})$$

where  $R$  and  $R_0$  are the final and initial dose rates,  $t$  is time in months, and  $\lambda$  is the decay constant (63 months for Co-60), predicts that the dose rate in the second case should be  $(2.1 \pm 0.1) \times 10^{17}$  ev/l-sec.

Because of the oxygen depletion effect the optical density versus time curve was not linear. This effect is quite evident in figure 9 for the irradiation time of 40 minutes. The initial two-thirds of the curve was, however, linear, and it was from this portion of the curve that the dose rates were determined.

The effect of chloride ion was tested in both of these studies. In each case it was found that the presence of  $10^{-3}$  M chloride ion had no detectable effect. We therefore conclude that, within the limits of detection, no organic impurities were present.

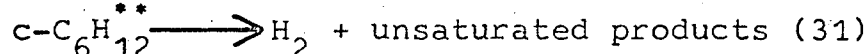
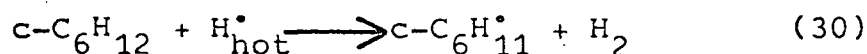
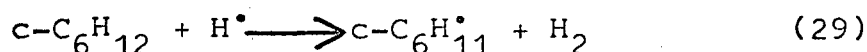
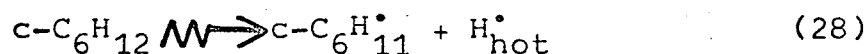
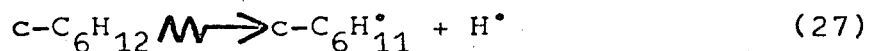
#### (b) The Cyclohexane Dosimeter

At very high dose rates the response of the Fricke

dosimeter falls. For example, Rotblat and Sutton<sup>24</sup> found  $G(\text{Fe}^{3+}) = 13.1 \pm 0.4$  at a dose rate of  $\sim 5 \times 10^{24}$  ev/l-sec. Since the manufacturer of the electron accelerator specified a dose rate of the order of  $10^{30}$  ev/l-sec., use of the Fricke dosimeter was not reasonable. There is a need for a chemical dosimeter that may be used at this dose rate.

The cyclohexane dosimeter may be such a chemical dosimeter. Burns and Parry<sup>60</sup> found that the yield of  $\text{H}_2$  from irradiated cyclohexane is essentially dose rate independent in the range  $10^{18}$  to  $10^{22}$  ev/l-sec. Indeed, dose rate and L.E.T. effects in cyclohexane are only observed in the presence of a radical scavenger, and such effects are not present initially<sup>61</sup>. Since the pulse of electrons used in this work is of such short duration, dose rate effects due to the formation of radical-scavenging products may be expected to be slight or non-existent.

The hydrogen formed in the radiolysis of cyclohexane has three sources - thermal hydrogen atoms, hot hydrogen atoms, and molecular processes<sup>62</sup>.



The  $\text{c-C}_6\text{H}_{12}^{**}$  is believed to be formed by ion neutral-

lization. The yields of hydrogen from these processes are:  $G(29) = 2.0$ ,  $G(30) = 0.85$ , and  $G(31) = 3.0$ . Values of  $G(H_2)$  from  $\gamma$  or electron irradiated cyclohexane that have been found are:  $(5.66 \pm 0.23)^{60}$ ,  $(5.85 \pm 0.08)^{62}$ ,  $5.44^{63}$ ,  $5.2^{64}$ , and  $5.4^{65}$ . This hydrogen represents about 99% of the products volatile at  $77^\circ K$ <sup>66,67</sup>, and hence it is an easily measurable product by ordinary vacuum techniques.

In radiation chemistry it is always wise to determine the effect of impurity upon the system yields when dealing with a pure system. To accomplish this three grades of cyclohexane were used - Phillips research, B&A reagent, and the middle one-third of distilled B&A reagent. As expected<sup>67</sup>, no difference was found in the hydrogen yields, within the error of the system ( $\sim 5\%$ ), for the three grades.

Since an unprecedented high dose rate was being used, it was necessary to determine if a dose rate effect existed. An attenuator was used to reduce the intensity of the beam to 5.5% of its uninterrupted value (as calculated from the area of the holes and the area of the uninterrupted beam). This attenuator was a 0.004" thick platinum disc in which were drilled forty-five 0.040" diameter holes arranged in a square pattern. The disc was placed one-half inch in front of the cell window. The attenuated yield was  $(1.1 \pm 0.2) \times 10^{-7}$  moles of hydrogen, which corresponds to  $(6.6 \pm 1.2) \%$  of

the unattenuated yield.

Electrons, which would be stopped by the attenuator if normal to it, may strike the edges of the holes at an angle other than the perpendicular, and in making such grazes would be reduced in energy but not stopped. The attenuated yield may be slightly high due to this. Also, with such small amounts of hydrogen the experimental errors may be as high as 15 to 20%.

With these two facts taken into account, the attenuated yield is quite close to that predicted by area calculations. Therefore the conclusion may be drawn that, within experimental errors and limitations just mentioned, no dose rate effect was evident in the hydrogen yields.

The total energy deposited in the stainless steel cell as determined by the cyclohexane dosimeter was  $(1.20 \pm 0.05) \times 10^{19}$  ev, assuming the value of  $G(H_2)$  of 5.66. Preliminary calorimetry studies confirm this value.

#### (c) Faraday Cup

Faraday cup measurements may be used to determine the number of electrons deposited in the system. By use of a variety of thickness of interposed material a transmission curve may be found, from which one may determine whether the electrons were mono- or multi-energetic.

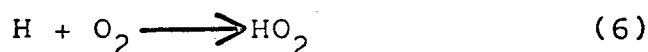
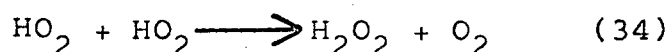
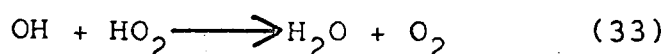
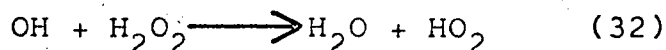
In the system used it was found that a 0.002" stainless steel window transmitted  $(2.6 \pm 0.3) \times 10^{13}$  electrons per pulse. This was  $\sim 57\%$  of the electrons incident upon the window. The transmission profile, using aluminum as the interposed material, was not characteristic of mono-energetic electrons, but rather that expected from multi-energetic electrons. This is the performance that would be expected since these electrons must pass through both the tube window and the cell window before reaching either the liquid in the stainless steel cell or the resistor in the Faraday cup.

Combining information from the cyclohexane dosimetry, and the Faraday cup measurements, and using the known penetration of these electrons, the average dose rate of the system is  $2.4 \times 10^{29}$  ev/l-sec. Due to variations of dose with depth and electron intensity during each pulse this dose rate may vary by a factor of  $\sim 25$ .

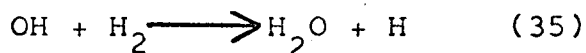
## RESULTS AND DISCUSSIONS

### 1. Cobalt-60 $\gamma$ Radiolysis

The nitrogen yields of aqueous nitrous oxide solutions have been determined as a function of solute concentration for various hydrogen ion concentrations for a total dose of  $7 \times 10^{17}$  ev/ml. (figure 4). Oxygen and hydrogen yields for these systems, having little meaning, have not been shown. Oxygen requires an induction period before it is formed <sup>29</sup>.



On the basis of these reactions oxygen must not be liberated until some hydrogen peroxide is formed. Hydrogen, on the other hand, may become involved in back reactions, such as



which will reduce its yield.

Experiments at doses lower than  $7 \times 10^{17}$  ev/ml. show greatly reduced oxygen yields, and higher hydrogen yields. Nitrogen yields were higher at very low doses, but at  $7 \times 10^{17}$  ev/ml. and doses  $\sim 1/10$  of that were markedly similar, showing differences well within experimental error. Neither the yield of hydrogen nor the yield of oxygen was dose independent, while the nitrogen yields were linear with dose for a

a total dose of  $7 \times 10^{17}$  ev/ml.

In the systems used no scavenger was added specifically for the hydroxyl radical. Its fate may be described by reactions (1), (3), (32), (33), and (35). It may also react with a solute, but such a reaction would be slow, since no good OH scavenger was used. Its fate is to produce  $H_2O$ ,  $H_2O_2$ ,  $O_2$ , or to reduce the yield of hydrogen.

#### (a) Neutral Solutions

The details of the neutral pH yields have been described elsewhere<sup>40</sup>; a two plateau curve is due to the scavenging of two species by nitrous oxide. About  $8 \times 10^{-5}$  M nitrous oxide is sufficient to scavenge the hydrated electron. From the yield of nitrogen in the first plateau, since each nitrogen molecule arises from one  $e^-_{aq}$ ,  $G_{aq}^- = 2.45 \pm 0.1$ . The second plateau is due to some species X, which may be the hydrogen atom. The 100 ev yield of X is  $0.65 \pm 0.1$ . These values are similar to those found in other systems (table II). This curve will be used as a standard with which others will be compared.

#### (b) Basic Solutions

The curves obtained in basic solution show at least three differences from the standard: 1) the sharp rise in  $G(N_2)$  occurs at solute concentrations one order of magnitude larger than in neutral solution; 2) the  $G(N_2)$  attained at  $2.6 \times 10^{-2}$  M nitrous



TABLE II

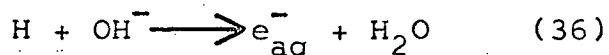
H-atom And  $e_{aq}^-$  Yields For A Variety Of Systems

SYSTEM	$G_{e_{aq}^-}$	$G_H$	REF.
$N_2O + H^+$	2.3		33
$N_2O + \text{isopropanol}$	$2.80 \pm 0.1$	0.60	31
$N_2O + \text{acrylamide}$	$2.80 \pm 0.15$		15
$N_2O + \text{ferrocyanide}$ $+ \text{ferricyanide}$	2.75		15
$N_2O + O_2 + \text{ferricyanide}$		$\sim 0.8$	44
$H_2O_2 + O_2$	2.85	$0.55 \pm 0.05$	45
$H_2O_2 + O_2$	$2.85 \pm 0.15$		46
$H_2O_2$	2.3	0.55	47
isopropanol + acetone	2.3	0.6	48
isopropanol + acetone	2.65	0.55	49
isopropanol + $H_2O_2$		$0.61 \pm 0.03$	50
$NO_3^- + HPO_3^-$	2.65	0.55	51
$HCO_3^- + O_2$	$2.3 \pm 0.1$	$0.75 \pm 0.1$	52
$C(NO_2)_4$	$2.6 \pm 0.26$		53
"many solutes"	2.3	0.55	54
AVERAGES	2.57	0.61	

oxide is much larger; and 3) the curves have only one plateau region.

The fact that the rise in the yield of nitrogen occurs at solute concentrations one order of magnitude higher may be due to a change in the chemical nature of the species scavenged, or the scavenger. Sufficient reason exists to believe that the scavenger's nature changes, but discussion on this is left until later. However, since  $\text{CO}_3^{=}$  was not removed from the alkaline solutions, and since no extensive investigation of the kinetics was undertaken, no conclusion may be drawn on this point.

The single rise in the pH 13 curve and the first rise in the pH 11.2 curve may be attributed to the reaction



which is known to occur in basic solution <sup>36,68</sup>. (The H-atom here used represents the species which is scavenged by high concentrations of nitrous oxide in neutral solution. Rather than argue the nature of this species it shall be designated as the H-atom hereafter, with the proviso that its exact nature is uncertain.) Since the hydrogen atom was the species responsible for the second rise at neutral pH, its conversion to the species to which the first rise was attributed would be expected to result in only one rise. The value of  $G(\text{N}_2)$  attained in this rise would be

expected, on the basis of the above argument, to be the  $3.1 \pm 0.1$  reached after both rises in neutral solution.

(i) pH 13

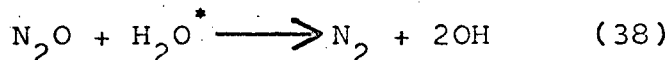
The value of  $G(N_2)$  at high nitrous oxide concentrations is much larger in basic than in neutral solution. This increment has previously been seen<sup>55</sup>, and is attributed to scavenging of excited water molecules by  $OH^-$ , which is in high concentration.



This would give a further number of hydrated electrons capable of reacting with nitrous oxide to yield  $N_2$ . The increment in  $G(N_2)$  reported was  $\sim 1$ , while that found in this experiment was  $\sim 1.6$ . Further investigation of this point was not undertaken.

(ii) pH 11.2

Since the  $OH^-$  concentration is  $\sim 60$  times less than at pH 13, intra-spur scavenging of excited water, as in reaction (37), would not be expected to occur. A more likely fate would be quenching, or direct reaction with nitrous oxide.



The rate constant of reaction (38) has been estimated to be 10 to 100 times less than that of reaction (15)<sup>55</sup>. Hence any rise in  $G(N_2)$  at pH 11.2 due to reaction of  $H_2O^*$  with nitrous oxide would occur at  $[N_2O]$  10 to 100 times larger than the rise due to reaction (15), assuming approximately equivalent steady state conc-

entrations of  $e_{aq}^-$  and  $H_2O^*$ . Just such behaviour is apparent; a two step curve is indicated.

Whether such an explanation may adequately account for the differences in nitrogen yields in these two basic solutions is entirely problematical. The investigation at pH 11.2 was not extensive enough to permit the drawing of any firm conclusions.

(c) pH 1.0

Since the  $[H^+] \geq 5[N_2O]$  in all cases, and  $k_{10}/k_{15} \sim 2$  (table I), all the scavengable  $e_{aq}^-$  will be transformed into H-atoms. The rise in  $G(N_2)$  should therefore take place in the same  $[N_2O]$  range as the second rise at neutral pH. This is approximately what is observed.

The yield of nitrogen at sufficiently high  $N_2O$  concentrations should be equal to  $G_{e_{aq}^-} + G_H$ . In neutral solution this sum was evaluated as  $3.1 \pm 0.1$ , and there is good reason to believe that it is higher in acidic solution<sup>15,28</sup>. While a value of 3.1 for  $G(N_2)$  is not quite attained, it is obvious that the curve is rising to at least that value.

The small yield of nitrogen seen at low nitrous oxide concentrations is real, and not due to degassing deficiencies. It appears that some species in low yield ( $G=0.35 \pm 0.05$ ) is being completely scavenged by  $3 \times 10^{-5}$  M nitrous oxide. An additional species has been noted in very acidic solution previously, and

identified as  $\text{H}_2^+$ <sup>28</sup>. The yield at pH 1.0 (taken from their graph) was 0.60. Whether one might draw the conclusion that the  $G(\text{N}_2) = 0.35$  may be equated with the  $G(\text{H}_2^+)$  reposted by Dainton and Peterson is open to debate.

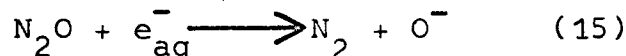
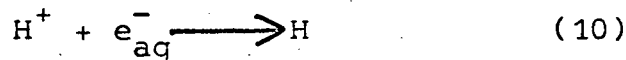
(d) Weakly Acidic Solutions

Nitrogen yields have been determined for acid solutions at pH 3.8, 4.0, 4.2, 4.3, and 4.5. The yields for 4.0, 4.2, and 4.5 have been included in figure 4. Comparison of these curves with neutral solution yields indicates that the abrupt rise in  $G(\text{N}_2)$  occurs at successively higher nitrous oxide concentrations as the hydrogen ion concentration is increased. The data for these five acidic solutions has been plotted as  $1/G(\text{N}_2)$  versus  $1/[\text{N}_2\text{O}]$  in figure 5. A linear relationship at each pH is evident. The common intercept occurs at  $G(\text{N}_2) = 2.4 \pm 0.1$ . The slopes of these lines, which is the mean  $[\text{N}_2\text{O}]/G(\text{N}_2)$  for each pH, is plotted as a function of hydrogen ion concentration in figure 6. Linearity is apparent at higher acidity, but is lost as the pH approaches seven.

(i) simple competition model

If the concentration of nitrous oxide is kept below  $\sim 2 \times 10^{-3}$  M, so that reaction (16) does not occur, then the only source of nitrogen is reaction (15). The effect of the abrupt rise occurring at higher nitrous oxide concentrations as the hydrogen

ion concentration increases may then be due to the reactions



competing. Thus the hydrogen ion concentration increase would necessitate an increase in the amount of nitrous oxide required to scavenge an equivalent number of hydrated electrons.

If the simple competition for hydrated electrons does in fact occur, then there existed an excellent opportunity of determining the rate constant ratio  $k_{10}/k_{15}$ . For reasons mentioned earlier, previous determinations of this ratio were perhaps invalid, or at least suspect. Thus the ratio found in this system would be of some value.

Since the limits of the first plateau in neutral solution were  $8 \times 10^{-5}$  and  $\sim 2 \times 10^{-2}$  M nitrous oxide, these were taken as the lower and upper limits of nitrous oxide concentrations used in this weakly acidic region. These limits exclude reaction (16), and yet all scavengable hydrated electrons are scavenged. The  $[\text{H}^+]$  necessary for a simple competition to occur, if the pulse radiolysis values of  $k_{10}$  and  $k_{15}$  are accepted, must be in the range  $3 \times 10^{-5}$  to  $2 \times 10^{-4}$  M.

Applying the steady state treatment to this simple competition, one finds

$$\frac{\text{Ge}_{\text{aq}}^-}{\text{G}(\text{N}_2)} = 1 + \frac{k_{10} [\text{H}^+]}{k_{15} [\text{N}_2\text{O}]} \quad (\text{xx})$$

This equation requires a linear relation between  $1/G(N_2)$  and  $1/[N_2O]$  at each pH, the  $1/G(N_2) = 0$  intercept is  $1/Ge_{aq}^-$  and the slope is  $k_{10}[H^+]/k_{15}$ . The value of  $Ge_{aq}^-$  then is  $2.4 \pm 0.1$ , which agrees well with the values found in neutral solution, and with those found in other work (table II). The rate constant ratios calculated from the slopes of the lines are not constant however, but decrease with pH - as shown in the following table.

TABLE III

Simple Competition Model Calculations

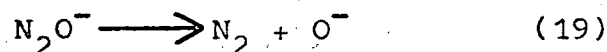
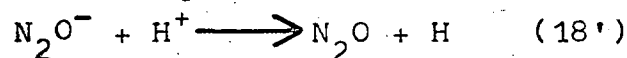
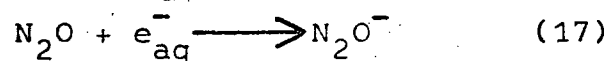
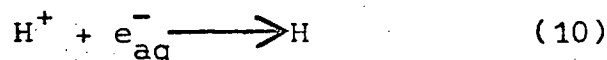
pH	$[H^+]$	Slope of Line or mean $[N_2O]/G(N_2)$	$k_{10}/k_{15}$
3.8	$1.7 \times 10^{-4}$	$7.2 \times 10^{-4}$	4.23
4.0	$1.0 \times 10^{-4}$	$4.0 \times 10^{-4}$	4.00
4.2	$6.0 \times 10^{-5}$	$2.0 \times 10^{-4}$	3.33
4.3	$4.8 \times 10^{-5}$	$1.2 \times 10^{-4}$	2.50
4.5	$3.2 \times 10^{-5}$	$4.5 \times 10^{-5}$	1.41

The model also predicts that the mean  $[N_2O]/G(N_2)$  is linear throughout the entire pH range, which figure 6 shows to be false. In ~~addition~~ addition the intercept of the linear curve should be zero, which is definitely not the case. One is therefore compelled to the conclusion that the simple competition model does not describe what has occurred.

(ii) charge transfer model

The suggestion of Dainton<sup>41</sup> and Anbar<sup>42</sup> that nitrous oxide might be involved in a charge

transfer process when a positively charged species is available looks to be a promising answer to this difficulty. The mechanism would then be



If the steady state assumption is made for  $\text{N}_2\text{O}^-$  and  $\text{e}_{\text{aq}}^-$ , then it follows that

$$\frac{\text{Ge}_{\text{aq}}^-}{\text{G}(\text{N}_2)} = \left(1 + \frac{k_{18}[\text{H}^+]}{k_{19}}\right) \left(1 + \frac{k_{10}[\text{H}^+]}{k_{17}[\text{N}_2\text{O}]}\right) \quad (\text{xxi})$$

With this scheme we have linearity of  $1/\text{G}(\text{N}_2)$  as a function of  $1/[\text{N}_2\text{O}]$ . However there is no common intercept; the intercept will depend upon  $[\text{H}^+]$  if charge transfer is to be important, which is to say that  $k_{18}[\text{H}^+]/k_{19}$  must be a significant factor. This is shown in table IV.

TABLE IV  
Charge Transfer Model Calculations

pH	calculated* intercept	actual intercept	difference
3.8	2.1±0.3	0.42±0.02	1.7±0.32
4.0	1.4±0.2	0.42±0.02	1.0±0.22
4.2	1.0±0.1	0.42±0.02	0.6±0.12
4.3	0.90±0.08	0.42±0.02	0.50±0.10
4.5	0.74±0.06	0.42±0.02	0.34±0.08

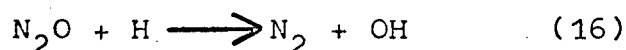
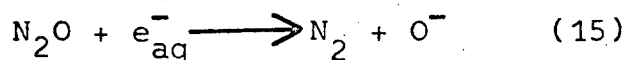
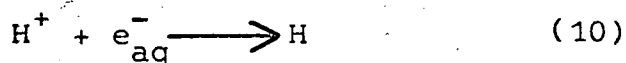
\* calculated from  $k_{18}/k_{19} = (2.6 \pm 0.4) \times 10^4$ , the average determined from the observed slopes, and assuming that  $k_{10}/k_{17} = 2.5$



The variation in the calculated intercepts is not seen experimentally, and is much too large to be experimental error. Thus the charge transfer mechanism also fails to adequately explain the experimental facts. Thus it too must be discarded.

(iii) H-atom scavenging model

A mechanism must be considered whereby reaction (16) which was thought to be excluded does in fact take place. This mechanism would be



Reaction (39) is one which is first order in H, and may or may not be a reaction with some other body.

Applying the usual steady state approximation

$$\frac{\text{Ge}_{\text{aq}}^-}{\text{G}(\text{N}_2)} = 1 + \frac{k_{10}k_{39}[\text{H}^+]}{k_{15}k_{16}[\text{N}_2\text{O}]^2 + k_{15}k_{39}[\text{N}_2\text{O}] + k_{10}k_{16}[\text{N}_2\text{O}][\text{H}^+]} \quad (\text{xxii})$$

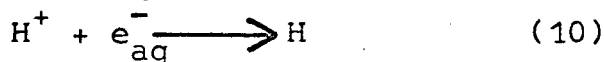
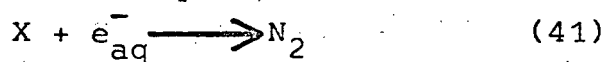
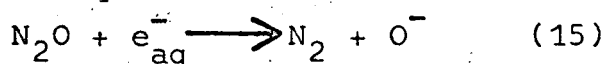
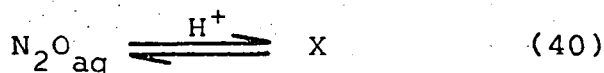
From this expression one may see that  $1/\text{G}(\text{N}_2)$  as a function of  $1/[\text{N}_2\text{O}]$  would not be linear unless

$k_{16}[\text{N}_2\text{O}]$  were much smaller than  $k_{39}$ . But if this were the case the equation would reduce to the simple competition equation - that is scavenging of H-atoms is not important. This mechanism must also be rejected.

(iv) solute chemical change model

The failure of the previous three models was

somewhat distressing. These results could not be explained on the basis of an ionic strength effect, since  $\mu \leq 2 \times 10^{-4}$  M in all cases. With this ionic strength the effect on  $k_{10}/k_{15}$  is less than 2%. The possibility of a change in the chemical nature of nitrous oxide in acidic solution was considered. The scheme of reactions is



where X is some acid species of nitrous oxide which reacts with the hydrated electron at a rate substantially different from that of  $\text{N}_2\text{O}$  in neutral solution. The kinetic equations applicable are

$$[\text{N}_2\text{O}]_t = [\text{N}_2\text{O}_{\text{aq}}](1 + K_{40}[\text{H}^+]) \quad (\text{xxiii})$$

$$\frac{\text{Ge}_{\text{aq}}^-}{G(\text{N}_2)} = 1 + \frac{k_{10}[\text{H}^+](1 + K_{40}[\text{H}^+])}{[\text{N}_2\text{O}]_t(k_{15} + K_{40}k_{41}[\text{H}^+])} \quad (\text{xxiv})$$

Equation (xxiv) predicts a common intercept of  $1/\text{Ge}_{\text{aq}}^-$ , and linearity of the  $1/G(\text{N}_2)$  versus  $1/[\text{N}_2\text{O}]$  function at each pH. The magnitude of  $k_{41}$  relative to  $k_{15}$  may be estimated from figure 6. At high pH  $k_{15}$  is the dominant term in the denominator and the slope found is less than the slope at low pH where  $K_{40}k_{41}[\text{H}^+]$  dominates. Since there is a reciprocal relation with these terms in equation (xxiv),  $k_{15} > k_{41}$ . Linearity of the  $[\text{N}_2\text{O}]/G(\text{N}_2)$  versus  $[\text{H}^+]$  function will occur

for two cases: 1)  $K_{40}[H^+] \ll 1$ , and 2)  $K_{40}[H^+] \gg 1$ . At very low hydrogen ion concentration  $[N_2O]/G(N_2)$  approaches zero. Thus this model adequately accounts for the experimental kinetic facts.

From the intercept of the  $1/G(N_2)$  versus  $1/[N_2O]$  curve  $Ge_{aq}^- = 2.4 \pm 0.1$ . The slope of the linear portion of the curve in figure 6, corresponding to  $K_{40}[H^+] \gg 1$ , is  $k_{10}/k_{41}Ge_{aq}^-$ . Assuming that  $k_{10} = (2.36 \pm 0.24) \times 10^{10} M^{-1}sec^{-1}$  and that  $Ge_{aq}^- = 2.4 \pm 0.1$ , then the value of  $k_{41}$  is  $(1.9 \pm 0.4) \times 10^9 M^{-1}sec^{-1}$ . By a series of successive approximations, assuming the values of  $Ge_{aq}^-$  and  $k_{10}$  mention above, and  $k_{15} = 9 \times 10^9 M^{-1}sec^{-1}$  (the pulse radiolysis value), values of  $K_{40}$  and  $k_{41}$  were found to be  $(6.0 \pm 0.5) \times 10^4 M^{-1}$  and  $(2 \pm 1) \times 10^9 M^{-1}sec^{-1}$  respectively. However a more accurate determination of  $k_{41}$  is from the slope of the  $[N_2O]/G(N_2)$  versus  $[H^+]$  curve. The values therefore are:

$$K_{40} = (6.0 \pm 0.5) \times 10^4 M^{-1}$$

$$k_{41} = (1.9 \pm 0.4) \times 10^9 M^{-1}sec^{-1}$$

This means that species X reacts with the hydrated electron five times more slowly than does  $N_2O$  in neutral solution.

If the chemical nature of  $N_2O$  is changing then it is possible that its absorption spectrum changes also. The absorption spectra of acidic, neutral, and basic aqueous atmospheric nitrous oxide solutions were determined on a Beckman DB spectrophotometer.

Only wavelengths greater than  $\sim 2100 \text{ \AA}$  could be investigated with this instrument. In basic solution an absorption was seen with a maximum at  $2160 \text{ \AA}$ . In both neutral and acidic solution a small absorption was seen at lower wavelengths. This absorption was still increasing at  $2100 \text{ \AA}$ , and appeared to be the tail of an absorption peak with a maximum at a lower wavelength. From the appearance of the absorptions the impression was gained that  $\lambda_{\text{max}}$  for neutral solution would be at higher wavelength than that for acidic solution, although it would be erroneous to positively state that such was the case. The shift in absorption maximum from basic to neutral solution, and the possible shift from neutral to acidic solution, tend to indicate that the chemical nature of nitrous oxide is pH dependent.

(e) The Nature Of X

(i) the hyponitrous acid hypothesis

The similarity of nitrous oxide to the isoelectronic and isosteric carbon dioxide is seen in table V. Furthermore, carbonic acid is much like hyponitrous acid in many respects (see table VI). Perhaps nitrous oxide may be converted to hyponitrous acid, much as carbon dioxide is converted to carbonic acid in aqueous solution. In the pH range studied the situation might be represented as

TABLE V

Comparison Of Some Of The Properties Of  $\text{CO}_2$  And  $\text{N}_2\text{O}$ \*

Property	$\text{CO}_2$	$\text{N}_2\text{O}$
melting point ( $^{\circ}\text{C}$ )	-56.6 (5.6 atm)	-90.8
boiling point ( $^{\circ}\text{C}$ )	-78.5	-88.5
solubility $25^{\circ}\text{C}$	0.75:1	0.50:1
(v:v of $\text{H}_2\text{O}$ ) $0^{\circ}\text{C}$	1.7:1	1:1
critical temperature	$31^{\circ}\text{C}$	$36.5^{\circ}\text{C}$
critical pressure	73 atm	71.7 atm
heat of fusion	45.3 cal/gm	36.5 cal/gm
heat of vapourization	~96 cal/gm	89.9 cal/gm
molecular shape	linear	linear
structure	$\text{O}=\text{C}=\text{O}$	$\text{N}^+=\text{N}^+=\text{O} \longleftrightarrow \text{N}^+ \text{N}^+=\text{O}^-$
bond distances	$\text{C}=\text{O}: 1.23 \text{ \AA}$	$\text{N}=\text{N}: 1.12 \text{ \AA}$ $\text{N}=\text{O}: 1.19 \text{ \AA}$
$S_{298}^{\circ}$ (cal/deg-mole)	51.061	51.44
$\Delta H_f^{\circ}$ (kcal/mole)	94.052	19.650
$\Delta F_f^{\circ}$ (kcal/mole)	94.260	24.930

\* from references 71, 73, and 74

TABLE VI

## Some Properties Of Carbonic Acid And Hyponitrous Acid\*

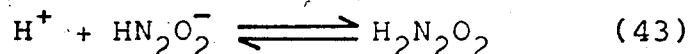
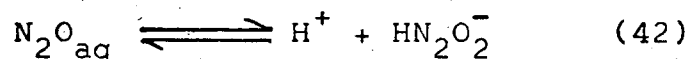
Carbonic Acid

1. Only 0.56% of  $\text{CO}_2$  in solution in form of  $\text{H}_2\text{CO}_3$ ; the greater part is only loosely hydrated.
2.  $\text{H}_2\text{CO}_3 \rightleftharpoons \text{H}^+ + \text{HCO}_3^-$   $k_{\text{apparent}} = 4.4 \times 10^{-7}$   
 $k_{\text{true}} = 4 \times 10^{-4}$
3.  $\text{HCO}_3^- \rightleftharpoons \text{H}^+ + \text{CO}_3^{2-}$   $k = 5 \times 10^{-11}$
4. The rate at which carbon dioxide comes to equilibrium with carbonic acid is measureably slow.

Hyponitrous Acid

1.  $\text{N}_2\text{O}$  is acid anhydride of  $\text{H}_2\text{N}_2\text{O}_2$ ; hyponitrous acid slowly decomposes to  $\text{N}_2\text{O}$ .
2.  $\text{H}_2\text{N}_2\text{O}_2 \rightleftharpoons \text{H}^+ + \text{HN}_2\text{O}_2^-$   $k = 9 \times 10^{-8}$
3.  $\text{HN}_2\text{O}_2^- \rightleftharpoons \text{H}^+ + \text{N}_2\text{O}_2^{2-}$   $k = 1 \times 10^{-11}$
4. Hyponitrous acid is about the same strength acid as carbonic acid (by electrical conductivity measurement).
5. It is such a weak acid that even HI is unaffected.
6. Main mode of decomposition of  $\text{H}_2\text{N}_2\text{O}_2$  with  $\text{H}_2\text{SO}_4$  present is to form  $\text{N}_2\text{O}$ : will decompose ~ 17% in 24 hours.
7.  $\text{N}_2\text{O} + \text{H}_2\text{O} \rightleftharpoons \text{H}_2\text{N}_2\text{O}_2$   $\Delta F_{298}^\circ = 42.76$  kcals from heats of formation of  $\text{N}_2\text{O}$  and  $\text{H}_2\text{N}_2\text{O}_2$ : this reaction is endothermic by 36.8 kcals.

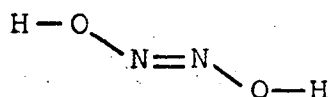
\* from references 70, 72, 74



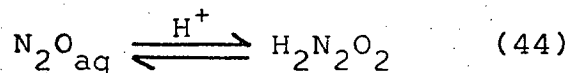
The structure of nitrous oxide is <sup>73</sup>



while that of hyponitrous acid is <sup>68,73</sup>



It is quite probable that, due to the changes in the configuration involved <sup>75,76</sup>,  $k_{43}$  is much greater than  $k_{42}$ . Now, because  $\text{N}_2\text{O}_{\text{aq}}$  and  $\text{H}_2\text{N}_2\text{O}_2$  are weak acids, equilibrium (42) will be much more slowly established than equilibrium (43). Since nitrous oxide is spontaneously formed from hydrogen hyponitrite, but not from hyponitrous acid <sup>75,77</sup>, then in a period too short for the establishment of a true equilibrium aqueous nitrous oxide in acid solution may be converted TEMPORARILY into hyponitrous acid. For this short period of time equilibria (42) and (43) may be represented by equation (44)



and we may write the following kinetic equations:

$$K_{44}[\text{N}_2\text{O}_{\text{aq}}][\text{H}^+] = [\text{H}_2\text{N}_2\text{O}_2] \quad (\text{xxv})$$

$$\begin{aligned} [\text{N}_2\text{O}]_t &= [\text{N}_2\text{O}_{\text{aq}}] + [\text{H}_2\text{N}_2\text{O}_2] \\ &= [\text{N}_2\text{O}_{\text{aq}}](1 + K_{44}[\text{H}^+]) \end{aligned} \quad (\text{xxvi})$$

It must be noted that equation (xxvi) is exactly the same as equation (xxiii) when X is  $\text{H}_2\text{N}_2\text{O}_2$ , and this will satisfy the kinetic equation (xxiv) which explains

the experimental facts. Because all of the experiments with nitrous oxide solutions were carried out no later than two hours after the preparation of the solution, this non-equilibrium hypothesis is plausible.

If hyponitrous acid, hydrogen hyponitrite, and hyponitrite ion were formed when nitrous oxide was dissolved in aqueous solution, then one might expect to see the absorption spectra of these species. The published absorption maxima are given in the following table.

TABLE VII

The Absorption Maxima Of  $\text{H}_2\text{N}_2\text{O}_2$ ,  $\text{HN}_2\text{O}_2^-$ , And  $\text{N}_2\text{O}_2^{=}$

Species	Absorption Maxima (nanometers)	Extinction Coeff.	Ref.
$\text{H}_2\text{N}_2\text{O}_2$	207		75
	208.5	2740	76
	242.5	122	76
$\text{HN}_2\text{O}_2^-$	232		75
	233	3310	76
$\text{N}_2\text{O}_2^{=}$	247		75
	248	3980	76

However, <sup>in</sup> the spectra of saturated aqueous nitrous oxide solutions at pH 1.0, 4.0, 7, and 13.0 no absorption peaks were exhibited at any of these wavelengths.

If  $\text{N}_2\text{O}$  and  $\text{H}_2\text{N}_2\text{O}_2$  are the analogs of  $\text{CO}_2$  and



$\text{H}_2\text{CO}_3$ , then one might expect that the pH dependence of the solubility of nitrous oxide would be similar to that of  $\text{CO}_2$ . The results of such experiments are shown in the following table VIII.

TABLE VIII

The Solubility Of Both Nitrous Oxide And Carbon Dioxide

Gas	Temp. (°C)	pH	Gas Pressure (torr)	Conc. in Sol. <sup>n</sup> (M x 10 <sup>2</sup> )	Solubility <sup>b</sup> (M/torr x 10 <sup>5</sup> )
N <sub>2</sub> O	23	1	214	0.74	3.5±0.3
N <sub>2</sub> O	24	7	220	0.77	3.5±0.3
N <sub>2</sub> O	21	13	350	1.1	3.2±0.3
N <sub>2</sub> O <sup>a</sup>	20	7	760	-	3.6
CO <sub>2</sub>	24	1	260	1.2	4.6±0.4
CO <sub>2</sub>	24	7	230	1.02	4.4±0.3
CO <sub>2</sub>	21	13	270	-	36
CO <sub>2</sub> <sup>a</sup>	24	7	760	-	4.6

a. taken from Handbook of Physics and Chemistry, 44th Ed.

b. error represent variation of 3 or 4 measurements

As may be seen nitrous oxide and carbon dioxide differ markedly in basic solution, but show similar behaviour in neutral and acid solution.

Whereas the solubility and spectral data were determined from solutions of concentration  $\geq 10^{-2}\text{M}$ , the radiolysis solutions were from 5 to 250 times more dilute. Thus it may not be surprising that in the time elapsed between the preparation and the

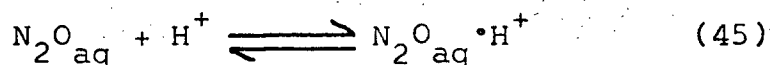
spectral determination of the solutions (~45 min.) only a very small percentage of the nitrous oxide in the concentrated solution would be converted into hyponitrous acid, while a relatively large per cent would be converted in the less concentrated solutions prepared for irradiation. Indeed it is normal to expect species to ionize to a greater extent when in dilute solution.

The spectral data indicates that very little  $\text{HN}_2\text{O}_2^-$  and  $\text{N}_2\text{O}_2^=$  are formed. The solubility data in basic solution also indicates that  $\text{N}_2\text{O}_2^=$  is not formed. While it may not be very surprising that little  $\text{HN}_2\text{O}_2^-$  exists in solution (analogy with  $\text{CO}_2$  suggests that very little  $\text{N}_2\text{O}$  in solution is in the form of  $\text{HN}_2\text{O}_2^-$ , which is to say that equilibrium (42) lies strongly to  $\text{N}_2\text{O}$  in neutral solution, and equilibrium (43) lies strongly to  $\text{H}_2\text{N}_2\text{O}_2$  in acid solution), it is perhaps surprising that no  $\text{N}_2\text{O}_2^=$  would form. Perhaps its formation is so slow that a long time is necessary before any reasonable amount forms.

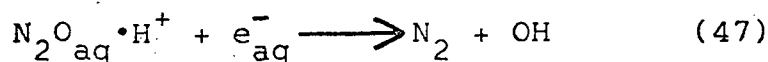
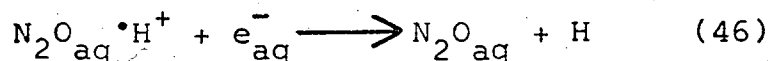
The conclusion that may be drawn from this assemblage of kinetic, spectral, and solubility data is that it would be presumptuous to identify species X as hyponitrous acid.

(ii) the hydration shell hypothesis

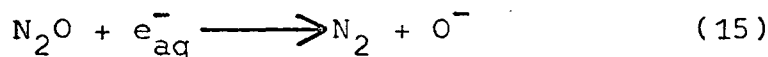
Species X may be a nitrous oxide molecule with a hydrogen ion in its hydration shell.



Such a species would not remove  $\text{H}^+$  from solution, as it would allow  $\text{H}^+$  to behave more or less as if it were "free". The acidity of the solution would not depend upon the nitrous oxide concentration. Its reactions with the hydrated electron would be to behave as if it were either  $\text{N}_2\text{O}$  or  $\text{H}^+$  as in (46) and (47).



which along with the individual reactions of  $\text{H}^+$  and  $\text{N}_2\text{O}$  with the hydrated electron



will result in the kinetic behaviour

$$[\text{N}_2\text{O}]_t = [\text{N}_2\text{O}_{\text{aq}}](1 + K_{45}[\text{H}^+]) \quad (\text{xxvii})$$

$$\frac{\text{Ge}_{\text{aq}}^-}{\text{G}(\text{N}_2)} = 1 + \frac{k_{10}[\text{H}^+](1 + K_{45}[\text{H}^+])}{[\text{N}_2\text{O}]_t(k_{15} + K_{45}k_{47}[\text{H}^+])} \quad (\text{xxviii})$$

only if  $k_{10} = k_{46}$ . This last equation satisfies the experimental facts.

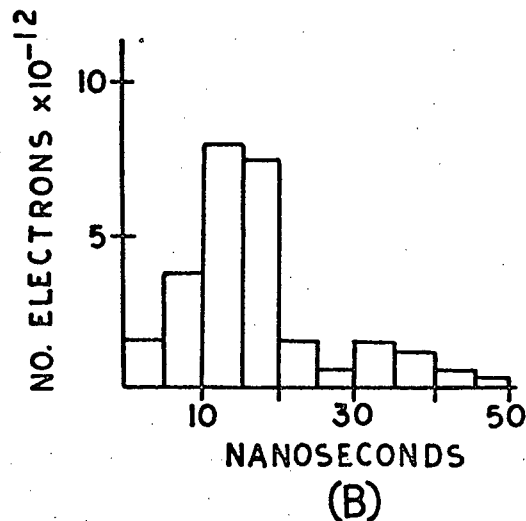
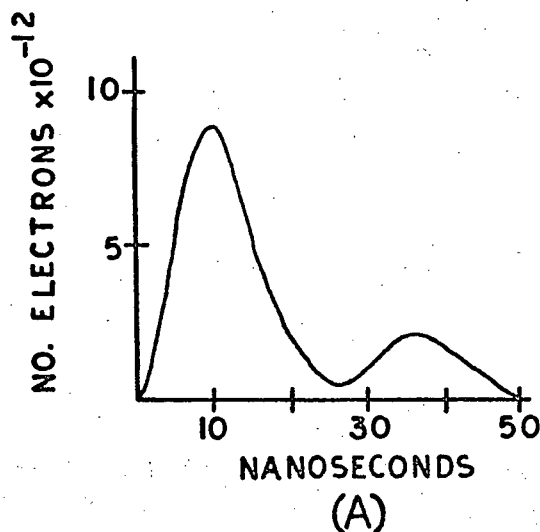
In such a system it would not be surprising that the solubility of the gas was independent of pH. The shift in the absorption maximum might be due to an ion atmosphere effect. However reaction (10) proceeds at a diffusion controlled rate; that is, each encounter of  $\text{H}^+$  with  $\text{e}_{\text{aq}}^-$  leads to reaction. Since  $\text{N}_2\text{O}_{\text{aq}} \cdot \text{H}^+$  must react with  $\text{e}_{\text{aq}}^-$  in two ways, and  $k_{42}$  must equal

$k_{10}$ , then it follows that  $N_2O_{aq} \cdot H^+$  must diffuse at a faster rate than  $H^+$  to be able to encounter  $e_{aq}^-$  more often. Since the hydrogen ion may diffuse by a proton transfer process, while the relatively bulky  $N_2O_{aq} \cdot H^+$  has no such mechanism available to it, it does not seem reasonable that  $N_2O_{aq} \cdot H^+$  is more mobile than  $H^+$ . The hydration shell hypothesis must, therefore, be considered a very unlikely mechanism.

## 2. Electron Irradiations

### (a) Diffusion Calculations

At the very high dose rates produced by the electron accelerator overlapping of the spurs is possible within  $\sim 10$  nanoseconds of their formation (i.e. before  $\sim 10^{-2}$  M  $N_2O$  is able to commence scavenging  $e_{aq}^-$ ). The time necessary for this overlap to occur must be known. From Faraday cup measurements the shape of the electron pulse in the cell environment is as shown in diagram (A). For the purposes of calculation (A) will be approximated by (B).



The radius,  $r$ , of the spur at time  $t$  is given by <sup>78</sup>

$$r = (r_0^2 + 2Dt)^{1/2} \quad (\text{xxix})$$

and the spur volume,  $V_s$ , by

$$V_s = [2\pi(2r_0^2 + 4Dt)]^{3/2} \quad (\text{xxx})$$

where  $D$  is the diffusion constant of the species under consideration, and  $r_0$  is the initial spur radius with respect to that species.

For the hydrated electron the initial spur radius is of the order of  $20 \text{ \AA}^{14}$ , while its diffusion constant is known to be  $4.75 \times 10^{-5} \text{ cm}^2/\text{sec}^{79}$ . On the basis of Faraday cup measurements and cyclohexane dosimetry, the average energy input per fast electron is estimated to be  $\sim 450 \text{ kev}$ . Assuming that it requires  $\sim 30 \text{ ev}$  to form a hydrated electron, then each fast electron will give rise to  $\sim 1.5 \times 10^4$  hydrated electrons on the average. For electrons with initial energy from 200 to 500 kev about 60% of the hydrated electrons formed are found in isolated spurs <sup>10</sup>. It is the overlap of these spurs that we wish to calculate. Since an electron of 500 kev will penetrate to a depth of  $\sim 2 \text{ mm}$  in water <sup>1b</sup>, and since the area irradiated was a circle 33 mm in diameter, then the volume irradiated was  $\sim 1.7 \text{ cm}^3$ . Taking into consideration the typical depth-dose pattern and the volume that will also be occupied by blobs and short tracks, then when the total volume of the isolated spurs

reaches  $\sim 2 \text{ cm}^3$  overlap should have occurred. Calculations done on the basis of the above assumptions are given in the following table.

TABLE IX

## Spur Overlap Calculations

pulse time (nanosec.)	r (Å)	V (Å <sup>3</sup> )	volume occupied (cm <sup>3</sup> )	60% volume (cm <sup>3</sup> )
5	20	$3.5 \times 10^5$	$8.2 \times 10^{-3}$	$4.9 \times 10^{-3}$
10	70	$1.5 \times 10^6$	$5.4 \times 10^{-2}$	$3.2 \times 10^{-2}$
15	100	$4.4 \times 10^6$	$2.3 \times 10^{-1}$	$1.4 \times 10^{-1}$
20	120	$7.6 \times 10^6$	$6.3 \times 10^{-1}$	$3.8 \times 10^{-1}$
25	140	$1.2 \times 10^7$	1.4	$8.4 \times 10^{-1}$
30	155	$1.7 \times 10^7$	2.5	1.5
35	170	$2.2 \times 10^7$	3.9	2.3
40	185	$2.8 \times 10^7$	5.4	3.2
45	195	$3.3 \times 10^7$	7.2	4.3
50	205	$3.9 \times 10^7$	9.3	5.6

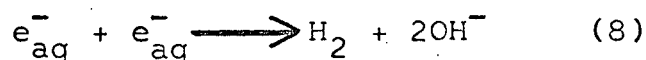
Even with all the approximations that were made (which usually erred on the generous side) it seems fairly obvious that overlap must have occurred by the time the pulse of electrons has finished. We are dealing therefore with a situation wherein homogeneous kinetics are applicable for a scavenging process in which  $(k_s[S])^{-1} \geq 3 \times 10^{-8}$  sec. (This was not the case for the cobalt-60  $\gamma$ -irradiations. With  $10^{-2}$  M nitrous oxide present only  $\sim 10$  tracks exist within the solution at any one time. This corresponds to a spur volume  $\sim 10^{-13}$  times the solution volume. Even

with only  $10^{-4}$  M  $N_2O$  and  $10^{-4}$  M  $H^+$  present the spur volume to solution volume ratio is  $\sim 10^{-10}$ :1. The kinetics of these cobalt-60  $\gamma$ -irradiations are definitely inhomogeneous.)

(b) Nitrogen Yields

The nitrogen yields for high intensity electron irradiations are shown in figure 7. The systematic error in all cases was  $\sim 12\%$ . Depletion of nitrous oxide is a very real possibility in the system. All the fast electrons are stopped in about  $1 \text{ cm}^3$  of  $10 \text{ cm}^3$  of solution, but the reactions that occur are completed so quickly that diffusion of  $N_2O$  from the bulk of the solution into the irradiation site is negligible. Depletion will be greater at lower concentrations of  $N_2O$ . This effect will cause points to be shifted horizontally by varying amounts, but the main features of the curve remain - a plateau and a sharp rise. By very generous estimation less than 25% depletion occurs at the lowest nitrous oxide concentration and less than 5% at the highest.

The nitrogen formed must (at least in part) be attributed to the reaction of  $N_2O$  with  $e_{aq}^-$  and with H-atoms. At high intensities the bimolecular reactions



compete with the reaction of nitrous oxide with these species much more effectively than at low intensity.

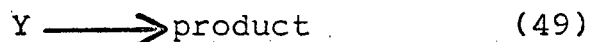
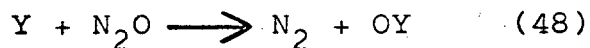
The effect, as predicted by equation (xviii), is the need of higher concentrations of  $N_2O$  to scavenge  $e_{aq}^-$  and H. Thus  $\sim 5 \times 10^{-4}$  M nitrous oxide is necessary to accomplish significant scavenging at high intensities whereas  $\sim 5 \times 10^{-5}$  M is sufficient at low intensities.

The variation of dose with depth as well as the variation of electron intensity during the pulse will result in a section of the irradiation site receiving a smaller dose at a rate much lower than the average. A lower dose rate means that homogeneity is a less likely condition. In this low dose rate section a condition of inhomogeneity may be found, such that less nitrous oxide is needed to scavenge  $e_{aq}^-$ . If this were the case, and if the section under discussion were a significant portion of the irradiation site, then a plateau could occur in the  $G(N_2)$  versus  $[N_2O]$  curve. As such a plateau is apparent in figure 7 at low  $N_2O$  concentrations, the above argument may be reasonable.

A most significant fact is that  $G(N_2)$  from a  $\sim 2 \times 10^{-2}$  M nitrous oxide solution is greater for the high intensity electron irradiations than for the low intensity cobalt-60  $\gamma$ -irradiations. This may be explained in two ways - either  $Ge_{aq}^-$  is, for some reason, higher at high intensity, or some other species contributes to this high value. If some other species reacts with  $N_2O$  at high intensity then it would also



be expected to do so at the same pH and  $[N_2O]$  in the cobalt-60 experiments.



If species Y is lost in reaction (49) by a pseudo-first order process, then reaction (48) would be intensity independent. If Y is lost by a bimolecular process then reaction (48) would produce less  $N_2$  at high intensity. The explanation of higher  $G(N_2)$  cannot be that another species is scavenged by  $N_2O$ .

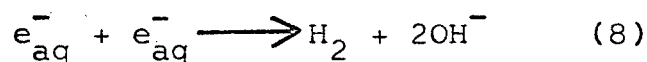
Therefore the conclusion that at high intensity  $Ge_{aq}^-$  is larger than at low intensity was drawn. Since  $N_2O$  is less effective in scavenging  $e_{aq}^-$  due to the bimolecular reaction of  $e_{aq}^-$  with itself, the same will be true of H-atoms. Significant scavenging of  $e_{aq}^-$  takes place an order of magnitude higher in nitrous oxide concentration at high intensity. Applying the same condition to the H-atom, scavenging of H will only just be significant in  $\sim 2 \times 10^{-2} M$   $N_2O$  solution. Thus an increase in  $G_H$  at high intensity would have only a small effect on  $G(N_2)$  at the nitrous oxide concentrations used. The increase in  $G(N_2)$  at high intensity must be attributed for the most part to an increase in  $Ge_{aq}^-$ . Whether  $G_H$  also increases may only be determined at pressures of  $N_2O$  greater than atmospheric. In any event, for  $[N_2O] \sim 2 \times 10^{-2} M$ ,  $G(N_2)$  at a dose rate of  $\sim 2 \times 10^{29}$  ev/l-sec. is greater than

at  $\sim 2 \times 10^{17}$  ev/l-sec. by approximately 0.4.

Addition of 0.26M isopropanol to a  $2.6 \times 10^{-2}$  M nitrous oxide solution does not reduce  $G(N_2)$  at these high intensities. Similar results have been reported at a dose of  $\sim 10^{17}$  ev/ml<sup>31</sup>. The conclusion to be drawn is that isopropanol does not scavenge a species capable of reacting with  $N_2O$  to form  $N_2$ . Since isopropanol is known to react much more rapidly with H than with  $e_{aq}^-$  there appears to be a real increase in  $Ge_{aq}^-$  in going from very low to very high dose rates.

### (c) Hydrogen Yields

The hydrogen is formed in the irradiations by reactions such as



where, since more  $e_{aq}^-$  is formed than H, reaction (8)

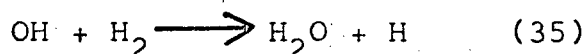
is the more important. The yield of hydrogen from pure water at high intensities was found to be

$G(H_2) = 1.15 \pm 0.2$ , which is similar to values found by others at high intensities<sup>25</sup>, and at low doses<sup>29</sup>.

This value of  $G(H_2)$  is lower than might have been expected on the basis of reactions (2) and (8) being the only significant processes. Then

$$G(H_2) = 1/2(Ge_{aq}^- + G_H) \geq 1.75 \pm 0.2 \quad (xxxi)$$

However hydrogen is lost in back reactions such as



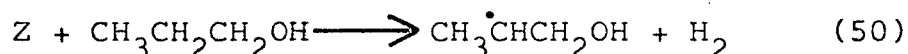
so that the yield of hydrogen is given by

$$G(H_2) \leq 1/2(Ge_{aq}^- + G_H - k_{35}[OH][H_2]/I) \quad (xxxii)$$

Thus a value of  $G(H_2) = 1.15 \pm 0.2$  is not surprising.

When nitrous oxide was introduced into the solution the hydrogen yield, as expected, was reduced. The reduction was proportional to the amount of  $N_2$  that was formed. The curve of  $G(H_2)$  versus  $[N_2O]$  (figure 8) is the reverse of figure 7, rising as  $G(N_2)$  falls. Since the hydrogen yield is not reduced to zero, it is evident that all the precursors of molecular hydrogen have not been scavenged, even at the highest  $[N_2O]$  used.

Addition of 0.26 M isopropanol to a solution of  $2.6 \times 10^{-2}$  M nitrous oxide increased the hydrogen yield by  $0.88 \pm 0.22$ . Since hydrogen may be formed from isopropanol by the abstraction of a H-atom by some species Z to give molecular hydrogen,



this increase must reflect the yield of Z. Thus we may say that  $G_Z = 0.88 \pm 0.22$ . One should note that this yield is higher than the  $G_H$  for cobalt-60 irradiations ( $G_H = 0.6$ ) and thus if Z is an H-atom the yield of both the primary reducing species H and  $e_{aq}^-$  increase at very high dose rates.

### 3. Conclusions

Cobalt-60  $\gamma$ -irradiations of aqueous nitrous oxide solution were undertaken in an attempt to determine yields of primary species produced by the radiation,

and to resolve differences in relative rate constant ratios of the type  $k(e_{aq}^- + S)/k(e_{aq}^- + N_2O)$ , which do not agree from place to place. These relative rate constant ratios are commonly determined with  $\sim 10^{-2}$  M  $N_2O$ . Use of this  $[N_2O]$  will result in additional unwanted scavenging of another species X, which will give erroneous ratios.  $G(X) = 0.65 \pm 0.1$ . Yields of primary species determined in this work are:  $Ge_{aq}^- = 2.4 \pm 0.1$ ,  $G_{H_2O}^* \sim 1.6$ , and  $G_{H_2^+} = 0.35 \pm 0.05$ .

Results from scavenging experiments in acidic dilute nitrous oxide solutions cannot be explained on the basis of a simple competition, a charge transfer mechanism, or scavenging of two distinct species. The results may, however, be explained by assuming that  $N_2O$  is converted to another species in acid solution. This acid nitrous oxide species reacts with the hydrated electron five times more slowly than does  $N_2O$  in neutral solution. It is suggested that this species might be  $H_2N_2O_2$ .

Neutral aqueous solutions of nitrous oxide were irradiated at high intensity with 0.52 Mev electrons in an effort to observe a decrease in solute reaction products, and to determine primary yields at high dose rates. As predicted, the concentration of  $N_2O$  necessary to achieve significant scavenging was larger at high dose rates than that at low dose rates. Since scavenging at low dose rates is complete for  $\sim 10^{-2}$  M  $N_2O$ ,

while at high dose rates it is not complete at  $2.6 \times 10^{-2}$  M  $\text{N}_2\text{O}$ , nitrous oxide seems to be less efficient at high intensities.

The high intensity yield of  $e_{\text{aq}}^-$  was found to be larger than the low intensity yield. A positive or negative statement of similar kind cannot be made for  $G_{\text{H}}$  until investigations at pressures of  $\text{N}_2\text{O}$  greater than atmospheric are completed. The yield of nitrogen from a  $2.6 \times 10^{-2}$  M  $\text{N}_2\text{O}$  solution at  $\sim 2 \times 10^{29}$  ev/l-sec. is higher ( $\Delta G(\text{N}_2) \sim 0.4$ ) than at  $\sim 2 \times 10^{17}$  ev/l-sec. The yield of hydrogen from pure water,  $G(\text{H}_2) = 1.15 \pm 0.2$ , is about that expected on the basis of the inter-spur reactions of  $\text{H}$ ,  $e_{\text{aq}}^-$ , and  $\text{OH}$ .

# REFERENCES

1. Much of this first section of the introduction was gleaned from the following:
  - (a) J.W.T. Spinks and R.J. Woods, An Introduction To Radiation Chemistry, John Wiley & Sons, New York, 1964 pp 15-76.
  - (b) G.J. Hine and G.L. Brownell, ed., Radiation Dosimetry, Acedemic Press, New York, 1956, pp 50-107.
  - (c) I.V. Vershchinskii and A.K. Pikaev, Introduction To Radiation Chemistry, English Translation from Isreal Program For Scientific Translations, Jerusalem, 1964, pp 6-16.
2. A.E. Moelwyn-Hughes, Physical Chemistry, Pergamon Press, Oxford, 1961, p 109.
3. L.I. Schiff, Phys. Rev., 1946, 70, 87; *ibid*, 1951, 83, 252
4. H.A. Bethe and J.A. Ashkin, in Experimental Nuclear Physics, (ed. E. Segre), Vol. 1, John Wiley & sons, New York, 1963, p 166 et seq.
5. W. Heitler, Quantum Theory Of Radiation, 3rd ed., Oxford University Press, 1954.
6. H.A. Behte, Ann. Physik, 1930, 5, 352
7. L. Katz and A.S. Penford, Rev. Mod. Phys., 1952, 24, 28
8. Vershchinskii and Pikaev, *op. cit.*, p 13.
9. A.O. Allen, The Radiation Chemistry Of Water And Aqueous Solutions, D.Van Nostrand, New York, 1961, p 3.
10. A. Mozumder and J.L. Magee, Rad. Res., 1966, 28, 203
11. A.O. Allen, *op. cit.*, p 12.
12. A.H. Samuel and J.L. Magee, J. Chem. Phys., 1953, 21, 1080
13. J.L. Magee, in Physical And Chemical Aspects Of Basic Mechanisms In Radiobiology, U.S. Natl. Res. Council, 1953, Publ. No. 305.

14. A. Kuppermann, in The Chemical And Biological Action Of Radiations, (M. Haissinski ed.), Vol.V., Acedemic Press, London, 1961, p 162.
15. F.S. Dainton and W.S. Watt, Proc. Roy. Soc., 1963, A275, 447
16. J.K. Thomas, Trans. Farad. Soc., 1965, 61, 702
17. U. Sokolov and G. Stein, J. Chem. Phys., 1966, 44, 2189
18. J.H. Baxendale and G. Hughes, Z. Physik Chem. [Frankfurt], 1958, 14, 323
19. E. Hayon and J.J. Weiss, Proc. Intern. Conf. Peaceful Uses At. Energy, 2nd, Geneva, 1959, Vol 29, p 80.
20. N.F. Barr and A.O. Allen, J. Phys. Chem., 1959, 63, 928
21. G. Czapski and Schwarz, J. Phys. Chem., 1962, 66, 471
22. J.W. Boag and E.J. Hart, Nature, 1963, 197, 45
23. J.P. Keene, Nature, 1963, 197, 47
24. J. Rotblat and H.C. Sutton, Nature, 1957, 180, 1332; Proc. Roy. Soc., 1960, A255, 490
25. J.K. Thomas and E.J. Hart, Rad. Res., 1962, 17, 408
26. A.R. Anderson and E.J. Hart, J. Phys. Chem., 1962, 66, 70
27. A.O. Allen, op. cit., p 96.
28. F.S. Dainton and D.B. Peterson, Proc. Roy. Soc., 1962, A267, 443
29. F.S. Dainton and D.C. Walker, Proc. Roy. Soc., 1965, A285, 339
30. G. Scholes and M. Simac, J. Phys. Chem., 1964, 68, 1731
31. J.T. Allen and C.M. Beck, J.A.C.S., 1964, 86, 1483
32. S. Ohno, Bull. Chem. Soc. Japan, 1965, 2018
33. F.S. Dainton and G.V. Buxton, Proc. Roy. Soc., 1965, A287, 427

34. F.S. Dainton and R. Rumfeldt, Proc. Roy. Soc., 1965, A287, 444
35. F.S. Dainton and P. Fowles, Proc. Roy. Soc., 1965, A287, 312
36. S. Gorden, E.J. Hart, M.S. Matheson, J. Rabani, and J.K. Thomas, Disc. Farad. Soc., 1963, 36, 193
37. J.P. Keene, Rad. Res., 1964, 22, 1
38. E.J. Hart and F.M. Fielden, in Solvated Electron, Am. Chem. Soc. Publ., Washington, 1965, pp 232-241
39. M. Anbar and P. Neta, Int. J. Applied Rad. and Isotopes, 1965, 16, 227
40. D. Head and D.C. Walker, Nature, 1965, 207, 517; D. Head, B.Sc. Thesis, 1965.
41. F.S. Dainton, Rad. Res. Supp. 4, p 72.
42. M. Anbar, in Solvated Electron, Am. Chem. Soc. Publ., Washington, 1965, pp 65-66
43. D.M. Brown, F.S. Dainton, J.P. Keene, and D.C. Walker, Proc. Chem. Soc., 1964, 266
44. G.E. Adams, J.W. Boag, and B.D. Michael, Trans. Farad. Soc., 1965, 61, 492
45. E. Hayon, J. Phys. Chem., 1964, 68, 1242
46. G. Czapski and A.O. Allen, J. Phys. Chem., 1962, 66, 471
47. E. Hayon, Trans. Farad. Soc., 1964, 60, 1059
48. J.T. Allen and G. Scholes, Nature, 1960, 187, 218
49. J. Rabani and G. Stein, J. Chem. Phys., 1962, 37, 1865
50. T. Sawai, Bull. Chem. Soc. Japan, 1966, 39, 955
51. M. Haissinski, J. Chim. Phys., 1965, 62, 1141
52. G. Scholes and M. Simac, Nature, 1963, 199, 276
53. J. Rabani, W.A. Mulac, and M.S. Matheson, J. Phys. Chem., 1965, 69, 53



54. E. Hayon, Trans. Farad. Soc., 1965, 61, 723
55. F.S. Dainton and S.R. Logan, Trans. Farad. Soc., 1965, 61, 715
56. H. Fricke and S. Morse, Am. J. Roentgenol. Radium Therapy, 1927, 18, 430; Phil. Mag., 1929, 7, 129, as cited in 9.
57. H.A.J.B. Battaerd and G.W. Tregear, Rev. Pure and Appl. Chem., 1966, 16, 83
58. A.O. Allen, op. cit., pp 20-23.
59. W.S. Moore, Physical Chemistry, 3rd ed., Prentice-Hall, Englewood Cliffs, N.J., 1962, pp 836-842.
60. W.G. Burns and J.R. Perry, Nature, 1964, 201, 814
61. P.J. Dyne and J.W. Fletcher, Can. J. Chem., 1960, 38, 851
62. L.S. Forrestal and W.H. Hamill, J.A.C.S., 1961, 83, 1535
63. W.H. Hamill and S.Z. Toma, J.A.C.S., 1964, 86, 1478
64. A.O. Allen and R.H. Schuler, J.A.C.S., 1955, 77, 507
65. R.H. Schuler, J. Phys. Chem., 1957, 61, 1472
66. J.W. Falconer and M. Burton, J. Phys. Chem., 1963, 67, 1743
67. H.A. Dewhurst, J. Phys. Chem., 1957, 61, 1472
68. J. Jortner and J. Rabani, J. Phys. Chem., 1962, 66, 2081
69. J.W. Mellor, A Comprehensive Treatise On Inorganic And Theoretical Chemistry, Longmans Green and Co., 1928, pp391-410.
70. W.L. Jolly, Inorganic Chemistry Of Nitrogen, Interscience, New York, 1964, p 71.
71. M.C. Sneed and R.C. Brasted, Comprehensive Inorganic Chemistry, Vol V, D. Van Nostrand, New York, pp 52-59.
72. Ibid. Vol VII, pp 42-49.

73. F.A. Cotton and G. Wilkinson, Advanced Inorganic Chemistry, Interscience, New York, 1962, pp 225, 254-260.
74. E.L. Quinn and C.L. Jones, Carbon Dioxide, Reinhold Publ. Corp., New York, 1936, pp 113-119.
75. J.R. Buchholz and R.E. Powell, J.A.C.S., 1963, 85, 509
76. M.N. Hughes and G. Stedman, J. Chem. Soc., 1963, 1239
77. J.H. Anderson, Analyst, 1963, 88, 494
78. A. Kuppermann, op. cit., p 112.
79. K.H. Schmidt and W.L. Buck, Science, 1966, 151, 70
80. Spinks and Woods, op. cit., p 6.
81. A. Kuppermann, op. cit., pp 150-154.

## LIST OF ILLUSTRATIONS









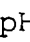
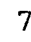





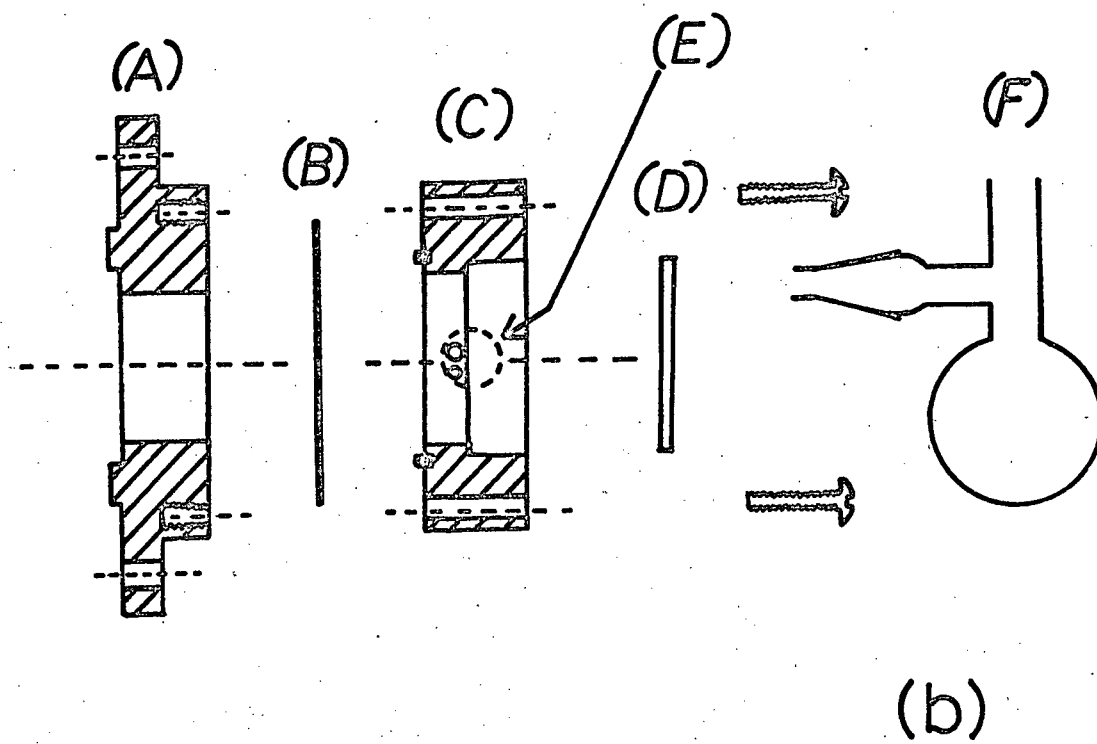
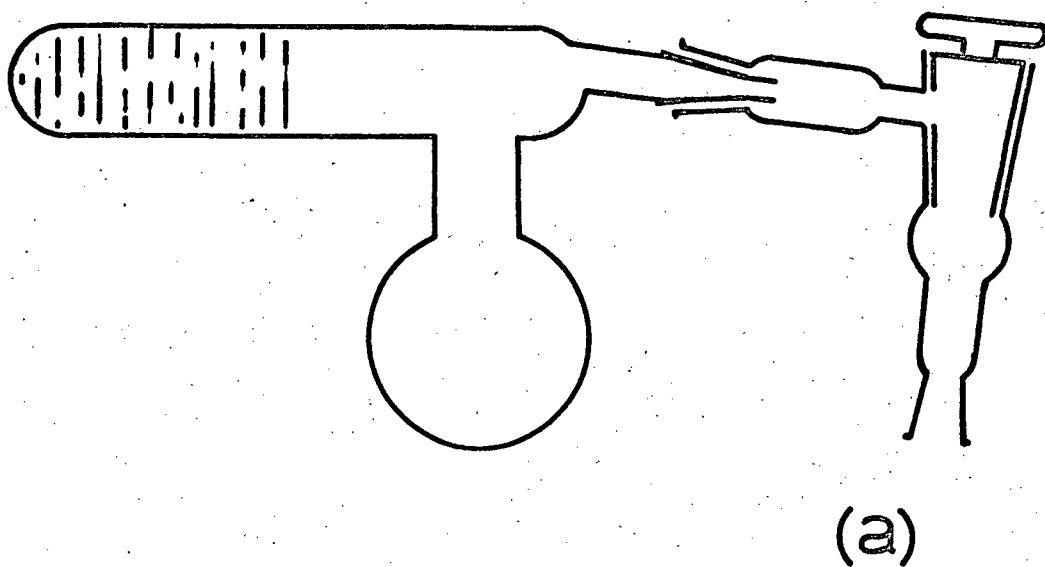
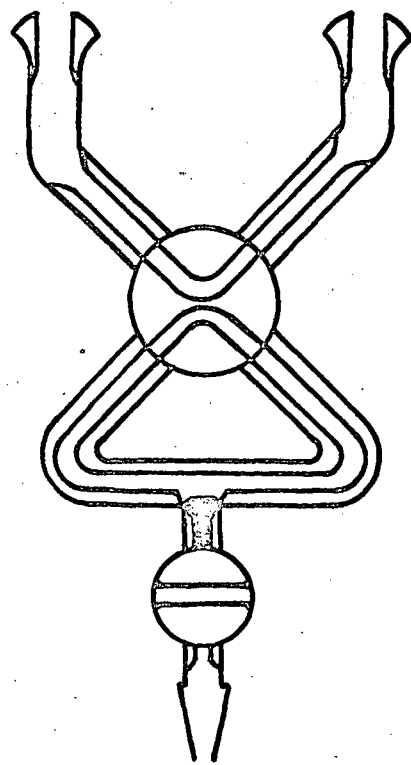
- Figure 1: a) Pyrex reaction vessel for gamma irradiations. Solutions prepared and degassed in 50 ml round-bottomed flask but irradiated in tube as shown. B14 ground glass joints were used.  
b) Vessel for electron irradiations. Aluminum face plate A attaches to accelerator; metal foil B transmits electrons into stainless steel cell C. Interior of C observed through pyrex window D araldited onto cell back. Solutions prepared and degassed in 50 ml round-bottomed flask F araldited onto cell at entrance port E.
- Figure 2: a) Cell for transfer of gases from vacuum line to gas chromatograph.  
b) Cross-section of Faraday cup used.
- Figure 3: Typical chromatogram.
- Figure 4: Nitrogen yields as a function of nitrous oxide concentration at various pH values for Co-60 gamma irradiations. Dose  $\sim 7 \times 10^{17}$  ev/ml. The pH's are:  1.0,  4.0,  4.2,  4.5,  7,  11.2, and  13.
- Figure 5: Reciprocal nitrogen yields as a function of reciprocal nitrous oxide concentrations for Co-60 gamma rays. Dose  $\sim 7 \times 10^{17}$  ev/ml.  pH 3.8,  pH 4.0,  pH 4.2,  pH 4.3,  pH 4.5, and  pH 7.
- Figure 6: Mean  $[N_2O]/G(N_2)$  as a function of hydrogen ion concentration.
- Figure 7: Nitrogen yields as a function of nitrous oxide concentration for electron irradiations. Dose  $\sim 1.2 \times 10^{19}$  ev/ml.  0.26 M isopropanol present,  no other solutes.

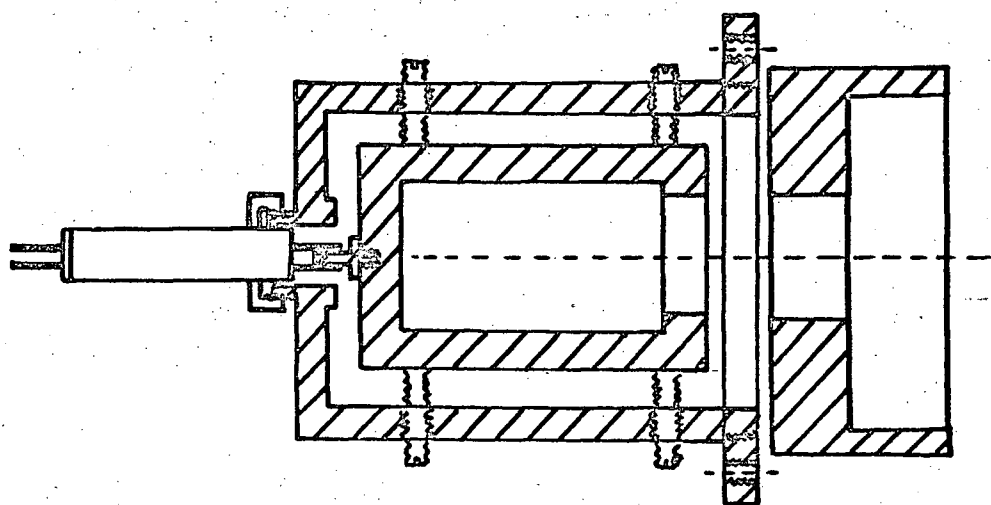
Figure 8: Hydrogen yields as a function of nitrous oxide concentrations for electron irradiations. Dose  $\sim 1.2 \times 10^{19}$  ev/ml. ○ 0.26 M isopropanol present, ● no other solute present.

Figure 9: Fricke Dosimetry plot. Optical density at 304 nanometers as a function of irradiation time. ○  $10^{-3}$  M chloride present. ● chloride absent.

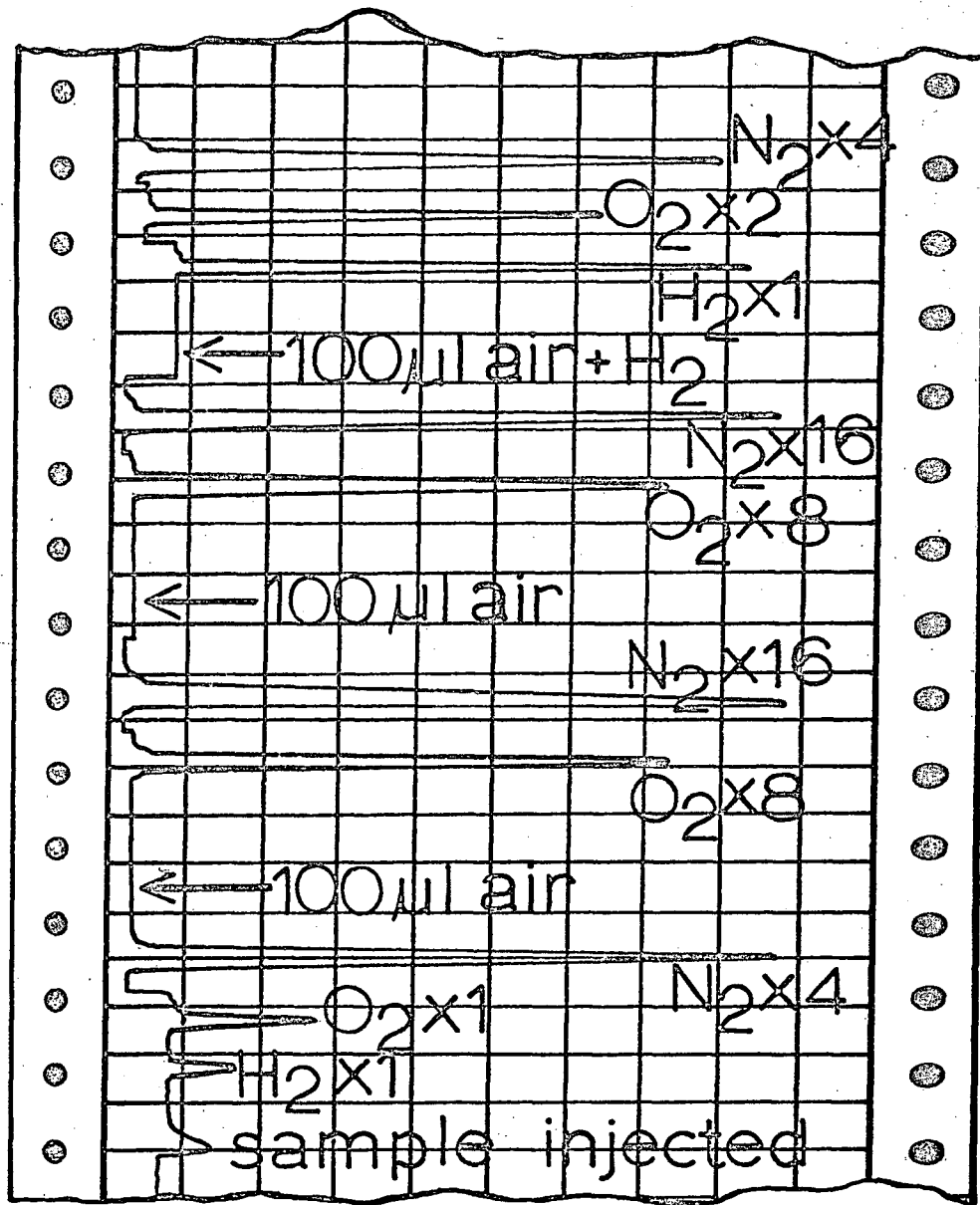


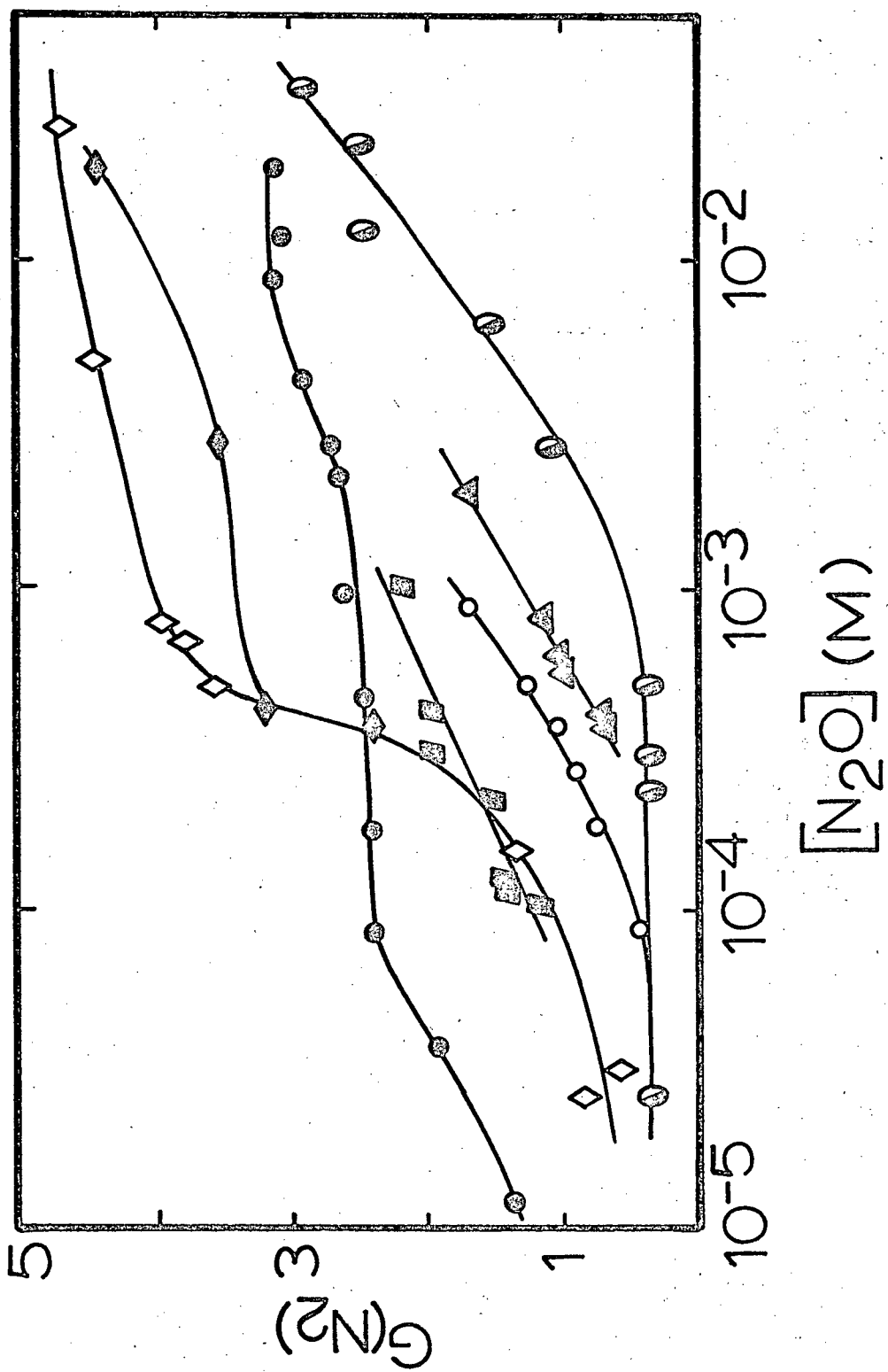


(a)

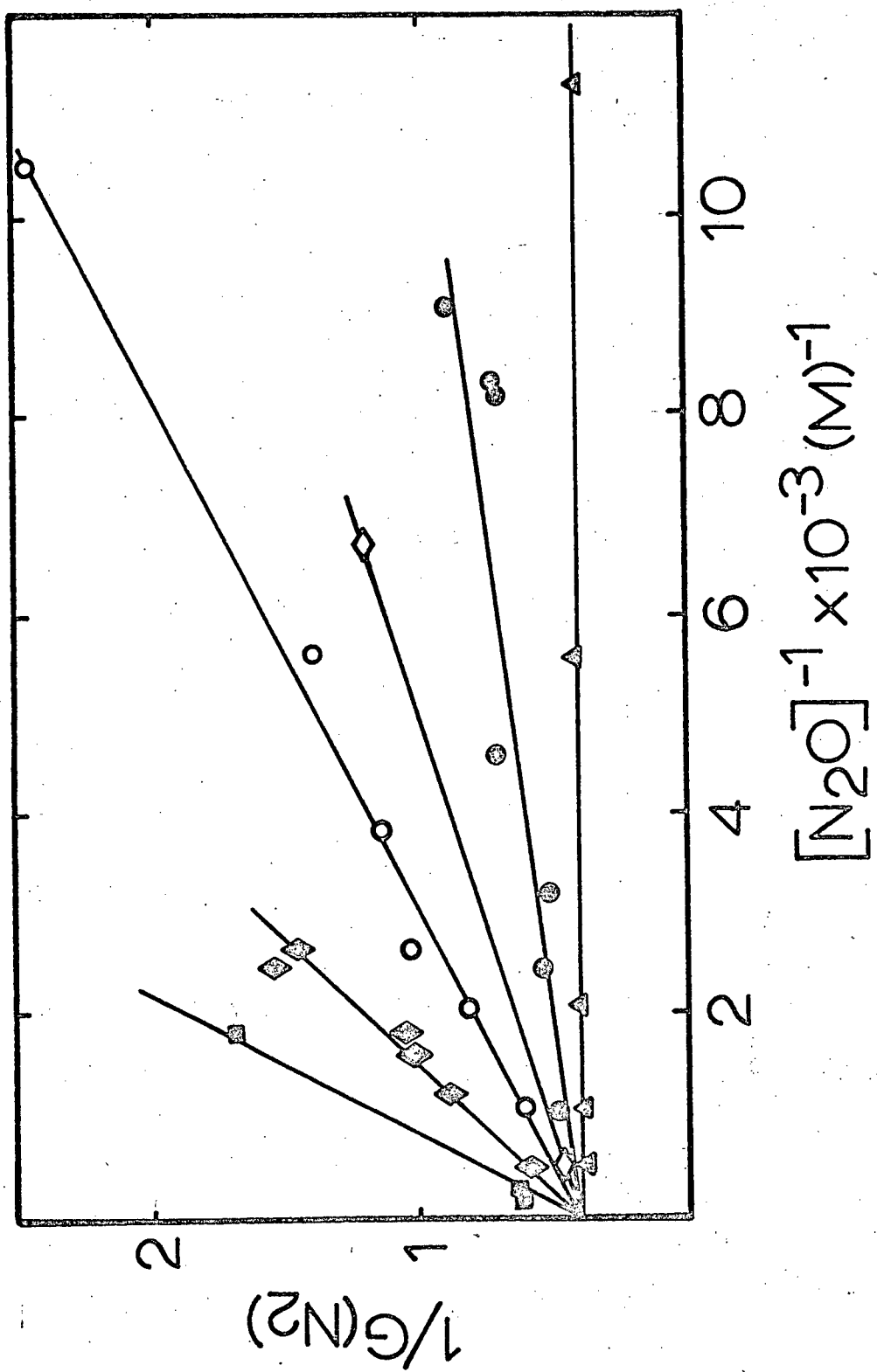


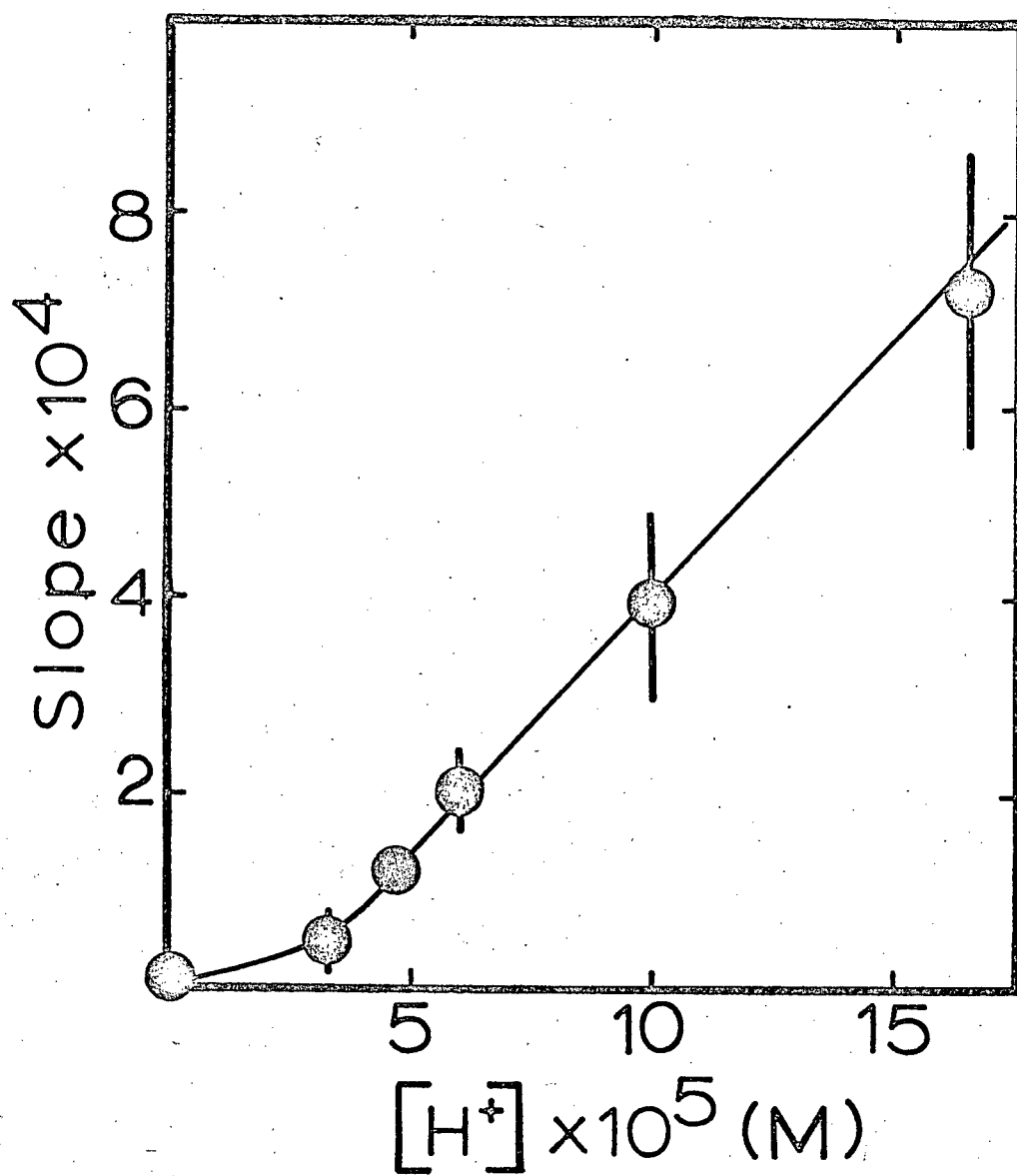
(b)

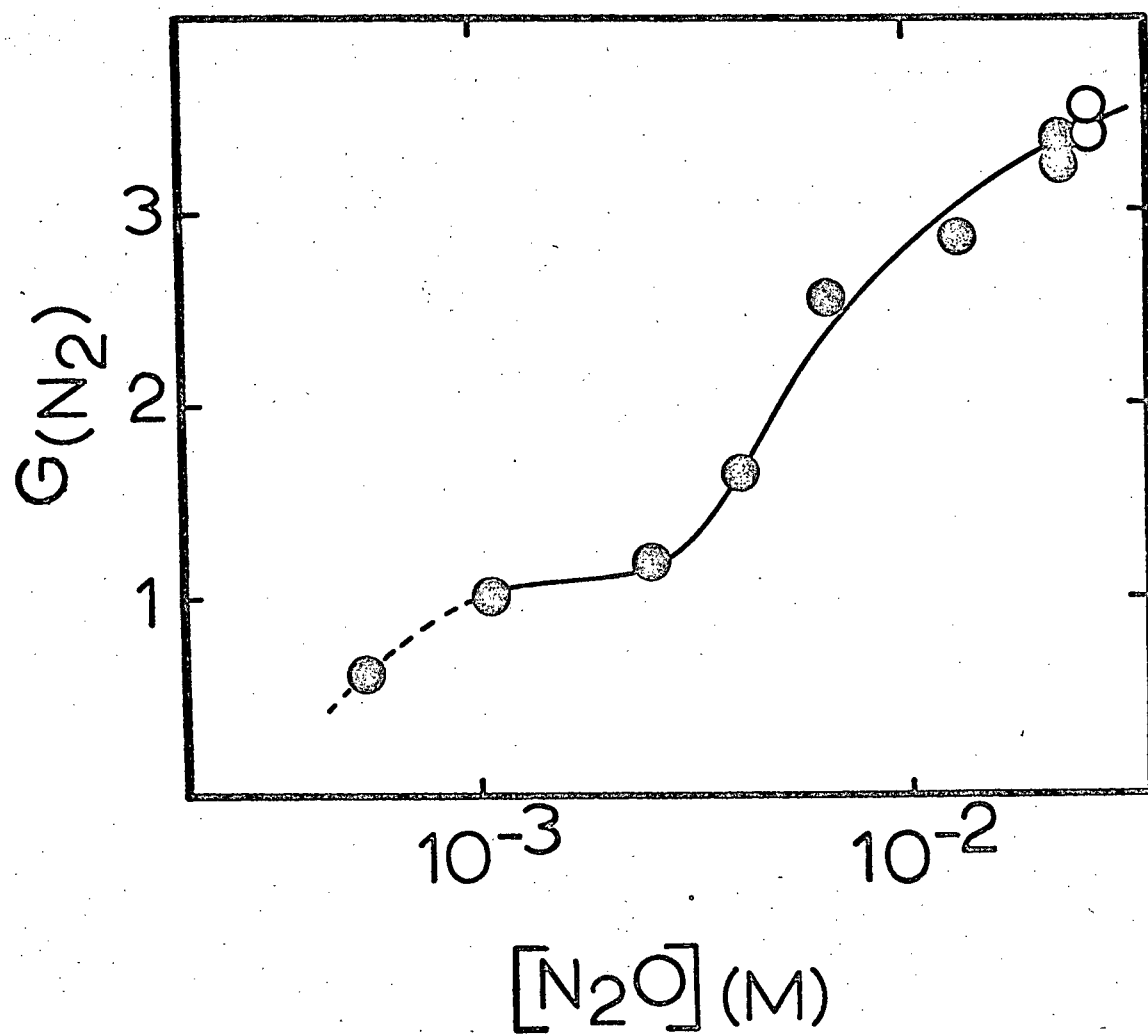


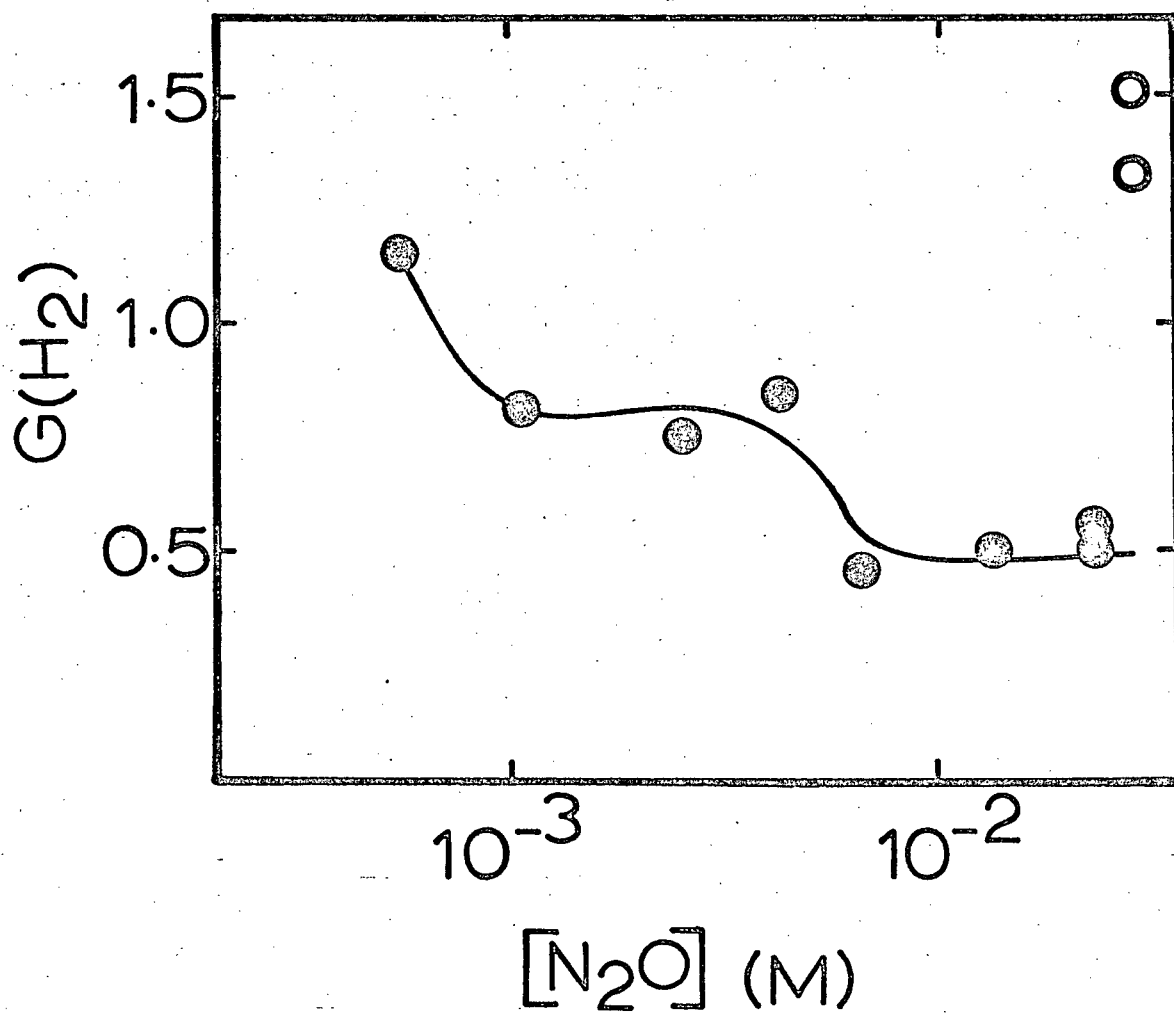


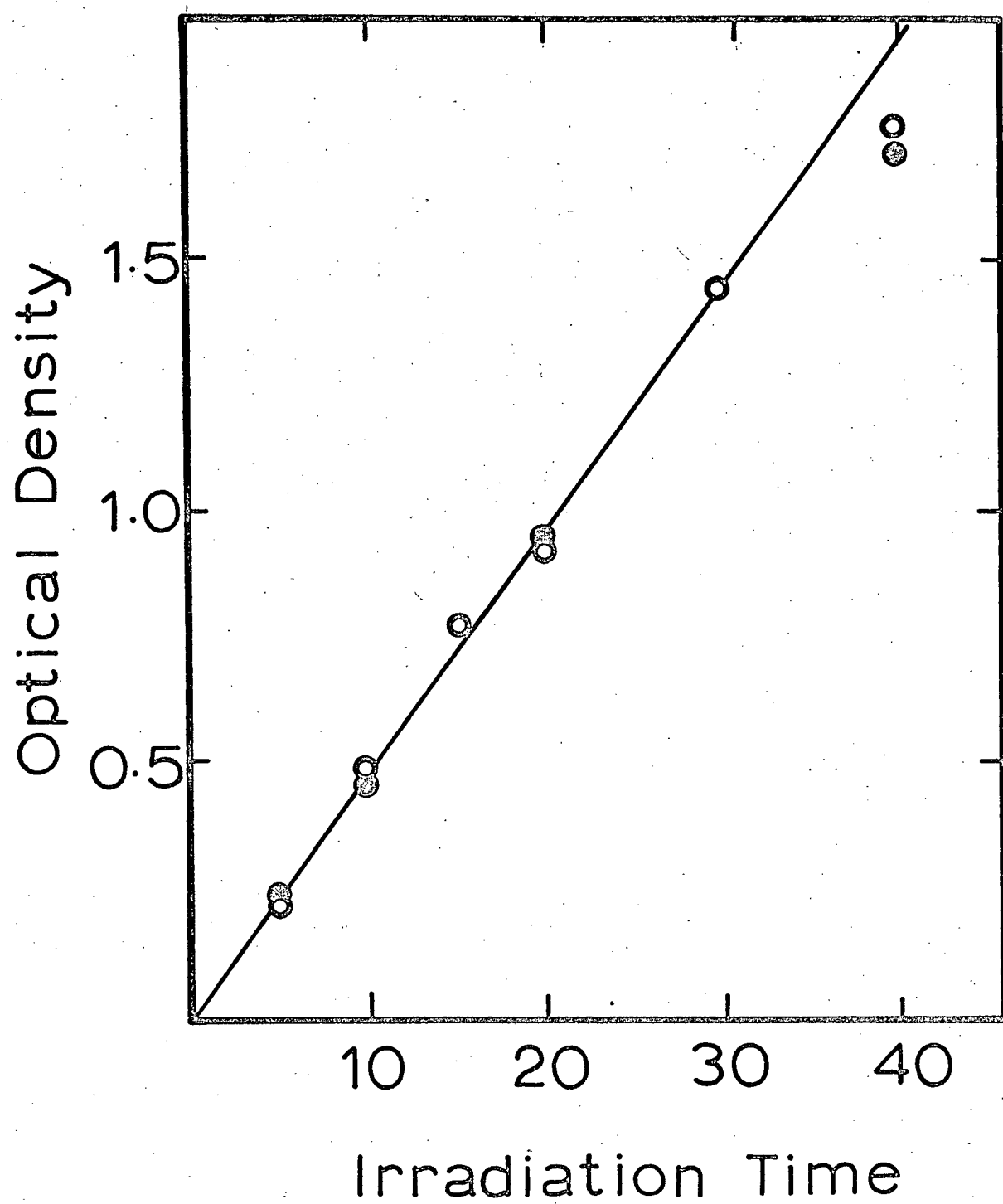












# LIST OF CORRECTIONS

Page	Line	Correction
5	4th last	elestic to read elastic
9	4th last	effect to read affect
10	2nd last	effect to read affect
11	7th	after chemical insert effect
17	3rd	$\text{ClCH}_3\text{COOH}$ to read $\text{ClCH}_2\text{COOH}$
18	8th	effect to read affect
20	2nd	(called scavenger) moved behind ution on 1st line
31	11th	was to read were
32	12th	surpress to read supress
35	8th last	it to read its
44	4th	reposted to read reported
45	10th	does to read did
56	table: b.	represent to read represents
58	last	$k_{42}$ to read $k_{46}$